

$^{59}\text{Cu}(p,\alpha)$ cross section for the heavy element nucleosynthesis in core collapse supernovae

Collaboration

R. Garg, C. Lederer-Woods, T. Davinson, M. Dietz,
D. Kahl, S. J. Lonsdale, A. Murphy, P. J. Woods

- *University of Edinburgh, UK*

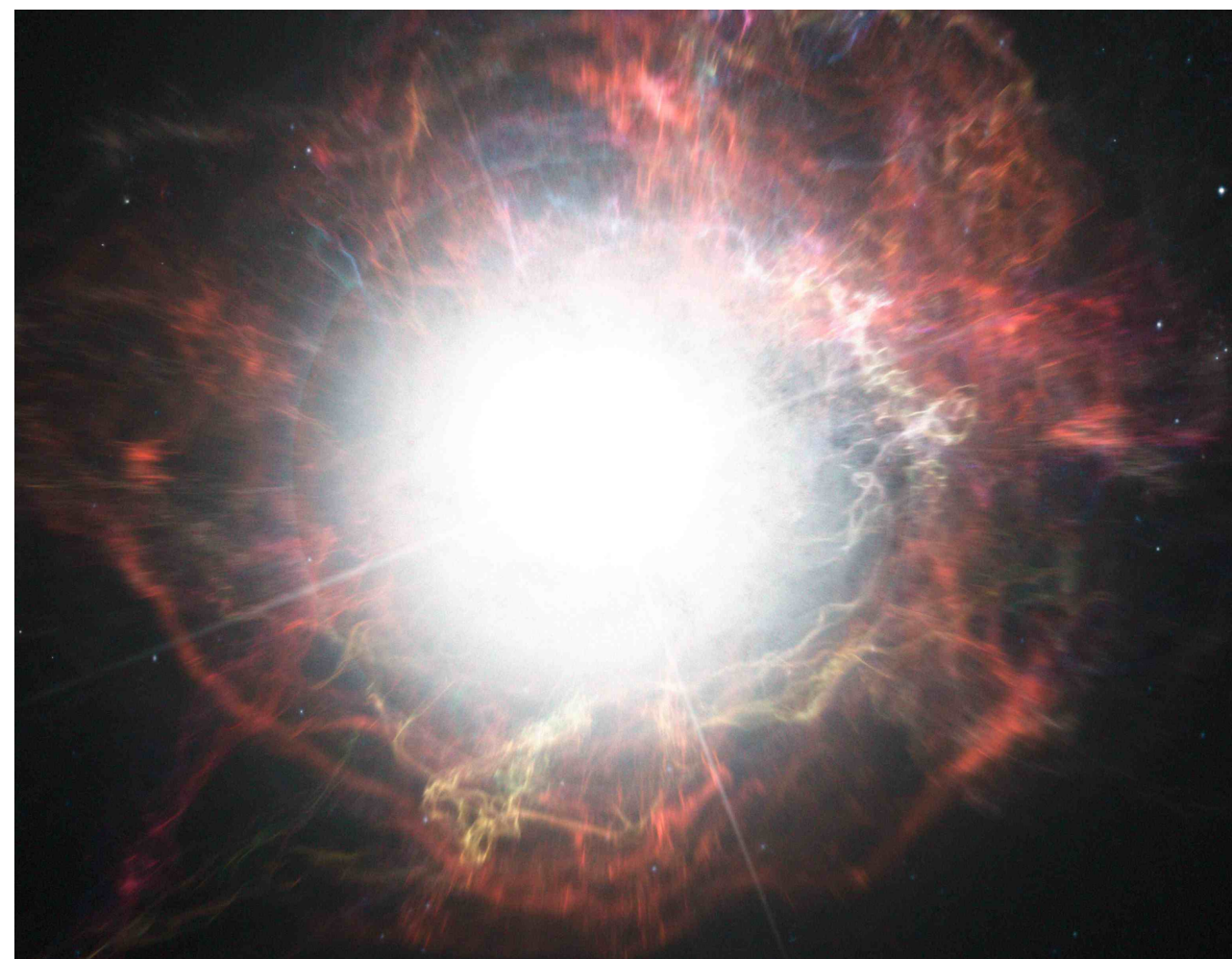
M. Barbagallo

- *CERN, Switzerland*

Astrophysical Motivation

Origin of heavy proton-rich nuclei

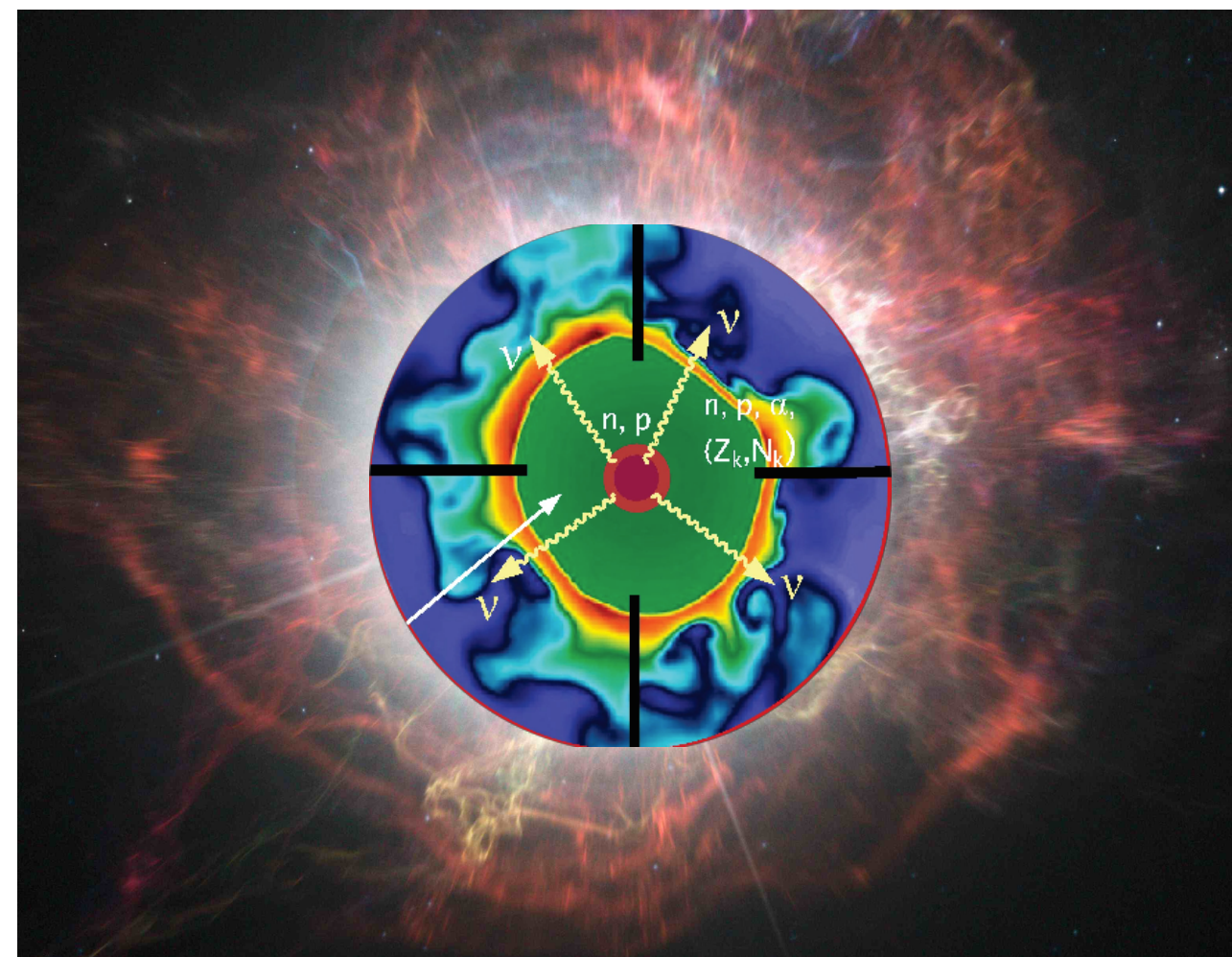
- The p-nuclei are thought to be produced via p-processes; proton-capture and photo disintegration of heavy nuclei.
- However, the observed abundance of some lighter p-nuclei ($^{92,94}\text{Mo}$ and $^{96,98}\text{Ru}$) not reproduced in most stellar models with these processes.



Astrophysical Motivation

Origin of heavy proton-rich nuclei

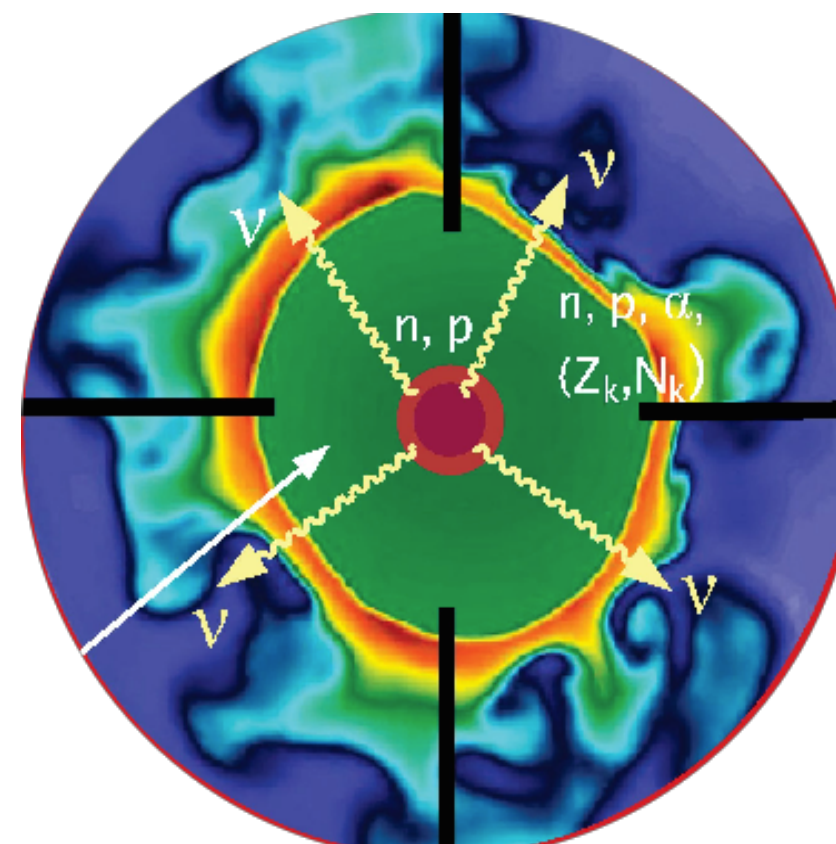
- The p-nuclei are thought to be produced via p-processes; proton-capture and photo disintegration of heavy nuclei.
- However, the observed abundance of some lighter p-nuclei ($^{92,94}\text{Mo}$ and $^{96,98}\text{Ru}$) not reproduced in most stellar models with these processes.
- Possible production of these p-nuclei in the vp-process in core collapse supernovae (*Fröhlich et al, PRL 96, 2006*)



Astrophysical Motivation

vp-process:

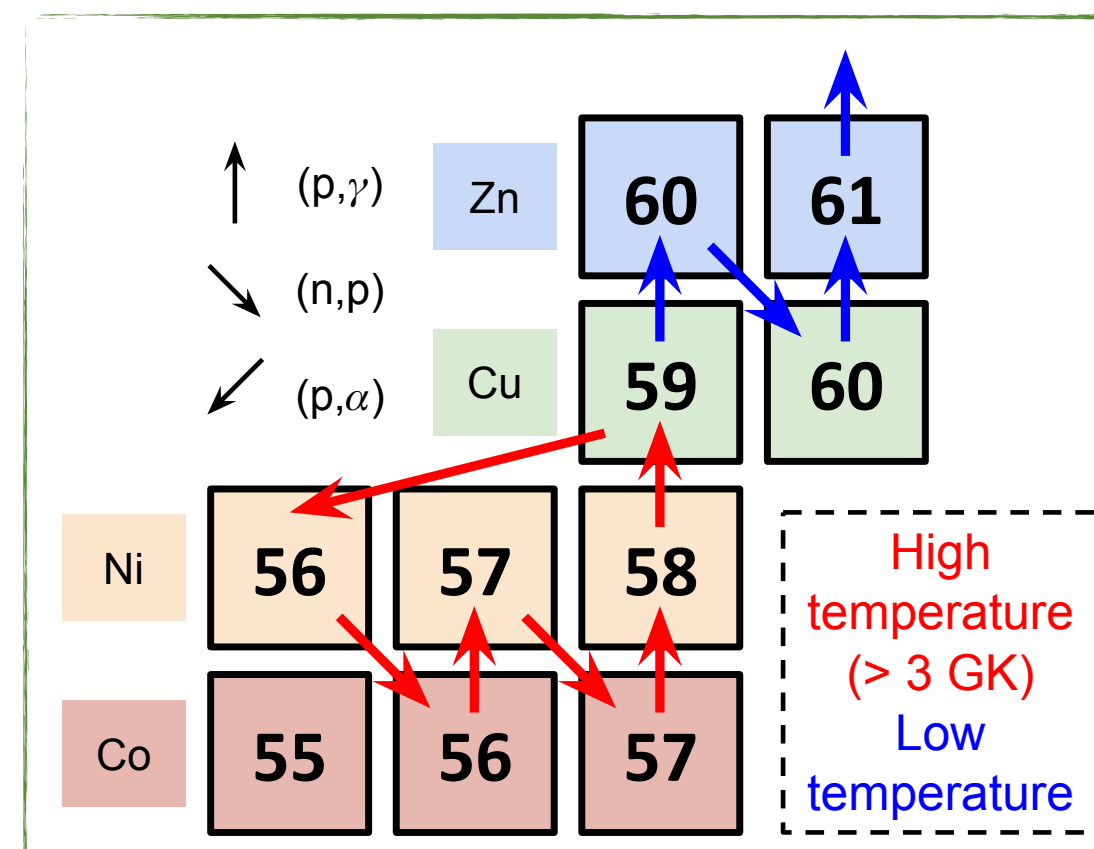
- The matter becomes proton-rich in core-collapse supernova by neutrino capture on free neutrons
- In this proton-rich ejecta, elements up to ^{64}Ge as proton captures probability drops at this point
- Antineutrino capture on protons can briefly cause a neutron density of $10^{14} - 10^{15} \text{ cm}^{-3}$
- These neutrons get captured on ^{64}Ge and unblock the matter flow to heavier element synthesis



Astrophysical Motivation

Origin of heavy proton-rich nuclei

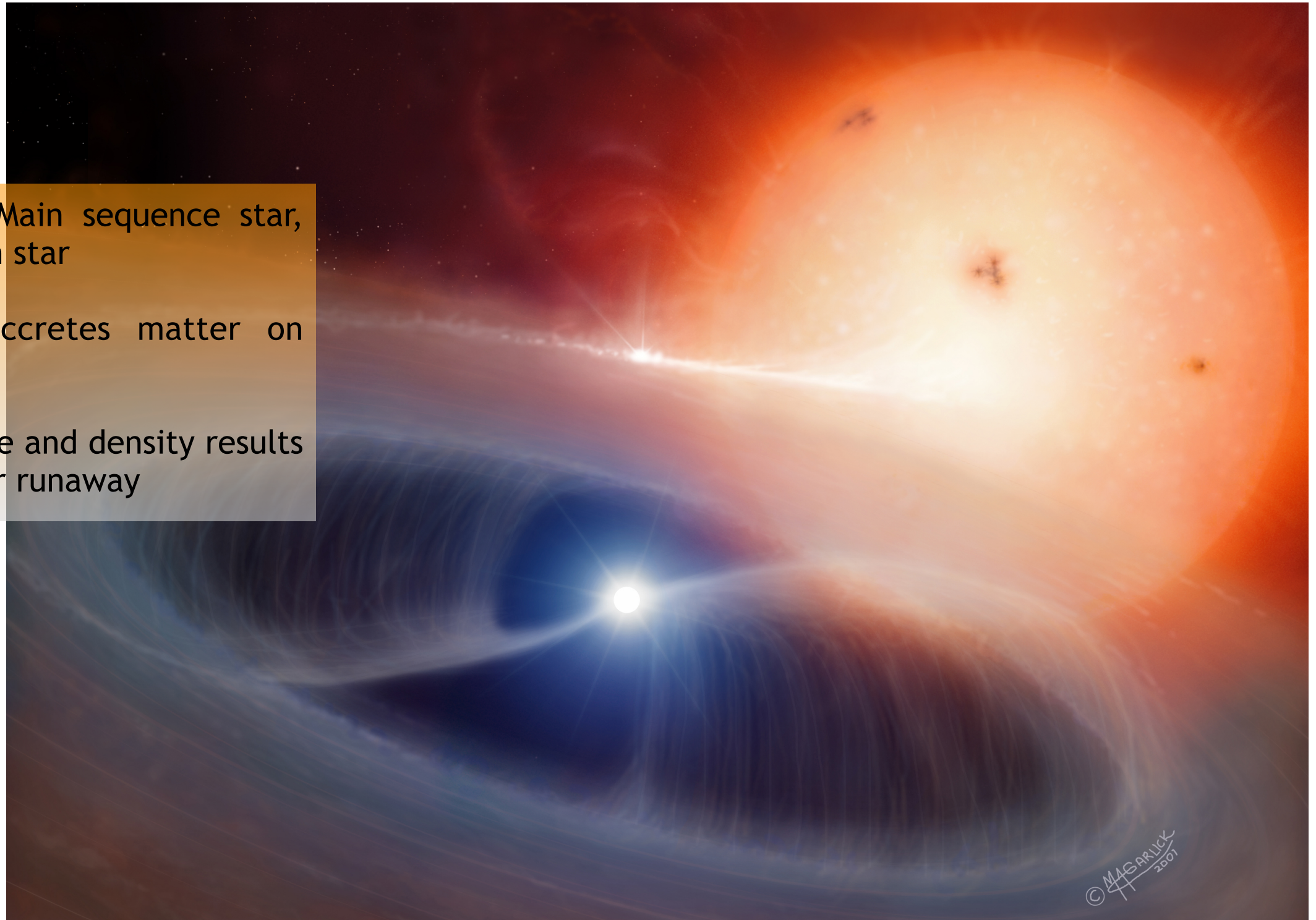
- NiCu cycle has been identified as the key end point at high temperatures (~ 3 GK)
(A. Arcones *et al*, *ApJ* 750, 2012)
- Competition between (p, α) and (p, γ) on ^{59}Cu sets temperature where heavy element formation starts
- Higher cross-over temperature = more efficient vp-process



Astrophysical Motivation

X-ray Bursts

- Binary system: Main sequence star, compact neutron star
- Neutron star accretes matter on surface
- High temperature and density results in thermonuclear runaway



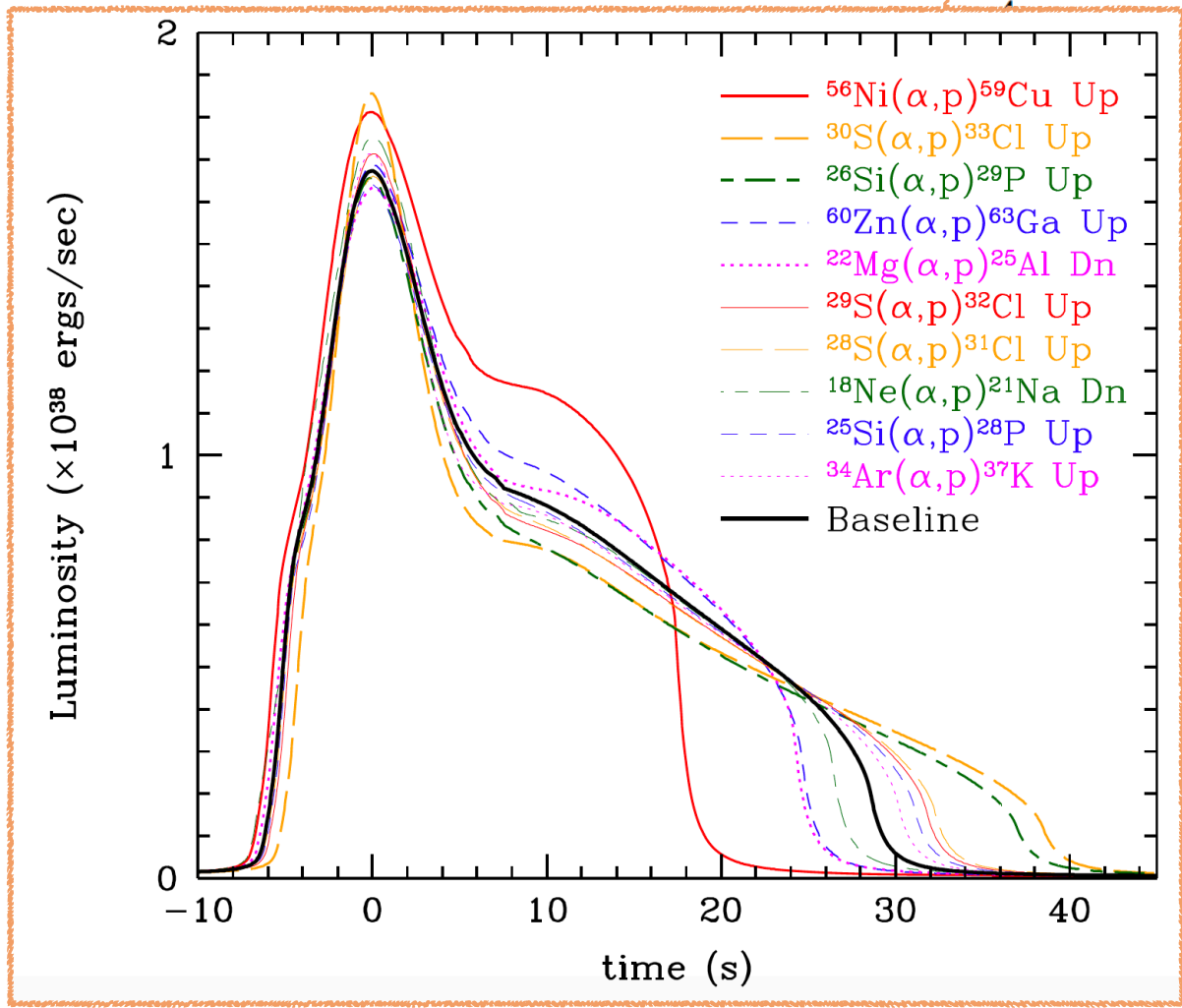
Astrophysical Motivation

X-ray Bursts (light curve)

- $^{59}\text{Cu}(p,\alpha)$ reaction is of key importance” for X-ray light curve
(*R. Cyburt et al, ApJ 830, 2016*)

Table 1
Reactions that Impact the Burst Light Curve in the Single-zone X-Ray Burst Model

Rank	Reaction	Type ^a	Sensitivity ^b	Category
1	$^{56}\text{Ni}(\alpha, p)^{59}\text{Cu}$	U	12.5	1
2	$^{59}\text{Cu}(p, \gamma)^{60}\text{Zn}$	D	12.1	1
3	$^{15}\text{O}(\alpha, \gamma)^{19}\text{Ne}$	D	7.9	1
	$^{30}\text{S}(\alpha, p)^{33}\text{Cl}$	U	7.8	1
	$^{26}\text{Si}(\alpha, p)^{29}\text{P}$	U	5.3	1
	$^{61}\text{Ga}(p, \gamma)^{62}\text{Ge}$	D	5.0	1
	$^{23}\text{Al}(p, \gamma)^{24}\text{Si}$	U	4.8	1
	$^{27}\text{P}(p, \gamma)^{28}\text{S}$	D	4.4	1
	$^{63}\text{Ga}(p, \gamma)^{64}\text{Ge}$	D	3.8	1
	$^{60}\text{Zn}(\alpha, p)^{63}\text{Ga}$	U	3.6	1



Single-zone model results

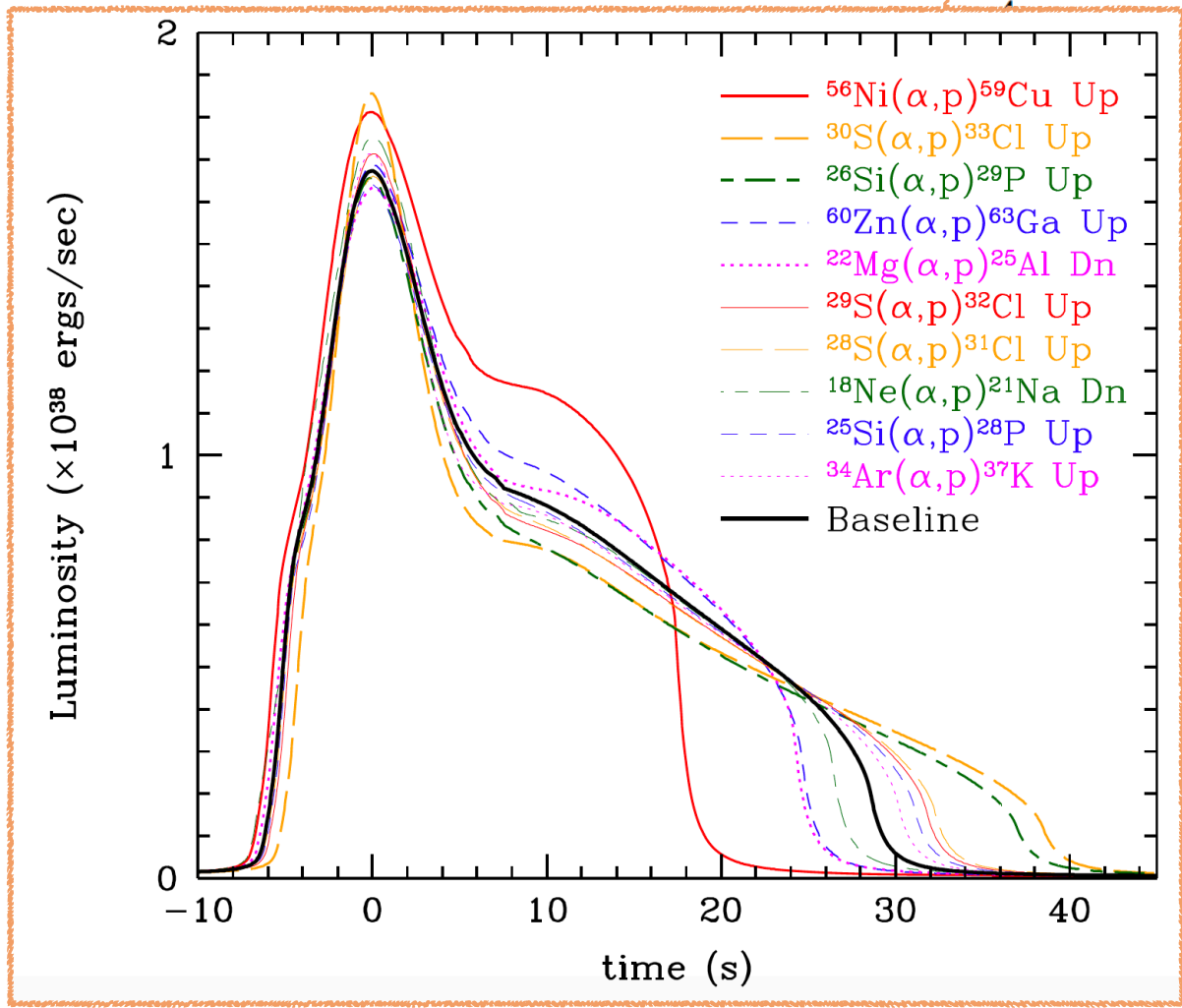
Astrophysical Motivation

X-ray Bursts (light curve)

- $^{59}\text{Cu}(p,\alpha)$ reaction is of key importance” for X-ray light curve
(*R. Cyburt et al, ApJ 830, 2016*)

Table 1
Reactions that Impact the Burst Light Curve in the Single-zone X-Ray Burst Model

Rank	Reaction	Type ^a	Sensitivity ^b	Category
1	$^{56}\text{Ni}(\alpha, p)^{59}\text{Cu}$	U	12.5	1
2	$^{59}\text{Cu}(p, \gamma)^{60}\text{Zn}$	D	12.1	1
3	$^{15}\text{O}(\alpha, \gamma)^{19}\text{Ne}$	D	7.9	1
4	$^{30}\text{S}(\alpha, p)^{33}\text{Cl}$	U	7.8	1
5	$^{26}\text{Si}(\alpha, p)^{29}\text{P}$	U	5.3	1
6	$^{61}\text{Ga}(p, \gamma)^{62}\text{Ge}$	D	5.0	1
7	$^{23}\text{Al}(p, \gamma)^{24}\text{Si}$	U	4.8	1
8	$^{27}\text{P}(p, \gamma)^{28}\text{S}$	D	4.4	1
9	$^{63}\text{Ga}(p, \gamma)^{64}\text{Ge}$	D	3.8	1
10	$^{60}\text{Zn}(\alpha, p)^{63}\text{Ga}$	U	3.6	1



Single-zone model results

Astrophysical Motivation

X-ray Bursts (light curve)

- $^{59}\text{Cu}(p, \alpha)$ reaction is of key importance” for X-ray light curve
(*R. Cyburt et al, ApJ 830, 2016*)

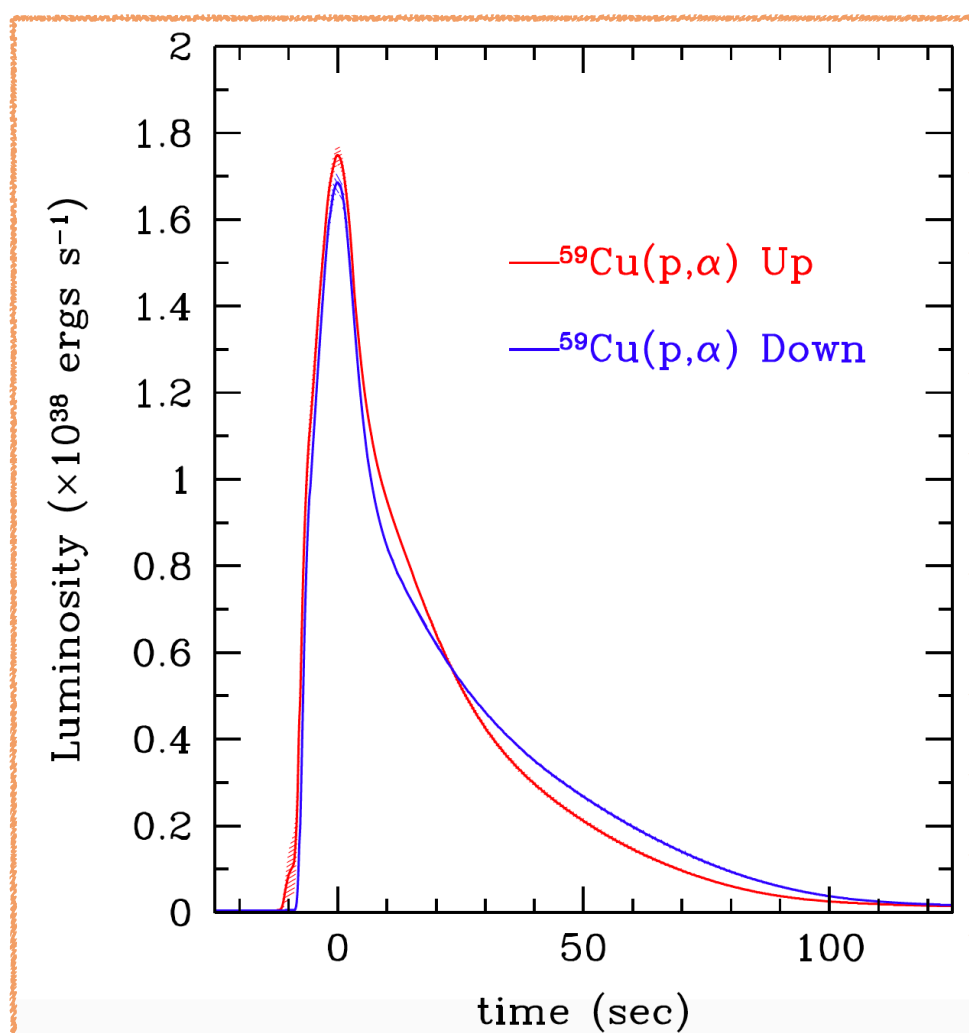


Table 2

Reactions that Impact the Burst Light Curve
in the Multi-zone X-ray Burst Model

Rank	Reaction	Type ^a	Sensitivity ^b	Category
1	$^{15}\text{O}(\alpha, \gamma)^{19}\text{Ne}$	D	16	1
2	$^{56}\text{Ni}(\alpha, p)^{59}\text{Cu}$	U	6.4	1
3	$^{59}\text{Cu}(p, \gamma)^{60}\text{Zn}$	D	5.1	1
4	$^{61}\text{Ga}(p, \gamma)^{62}\text{Ge}$	D	3.7	1
5	$^{22}\text{Mg}(\alpha, p)^{25}\text{Al}$	D	2.3	1
6	$^{14}\text{O}(\alpha, p)^{17}\text{F}$	D	5.8	1
7	$^{23}\text{Al}(p, \gamma)^{24}\text{Si}$	D	4.6	1
8	$^{18}\text{Ne}(\alpha, p)^{21}\text{Na}$	U	1.8	1
9	$^{63}\text{Ga}(p, \gamma)^{64}\text{Ge}$	D	1.4	2
10	$^{19}\text{F}(p, \alpha)^{16}\text{O}$	U	1.3	2

Multi-zone model results

Astrophysical Motivation

X-ray Bursts (light curve)

- $^{59}\text{Cu}(p, \alpha)$ reaction is of key importance” for X-ray light curve
(*R. Cyburt et al, ApJ 830, 2016*)

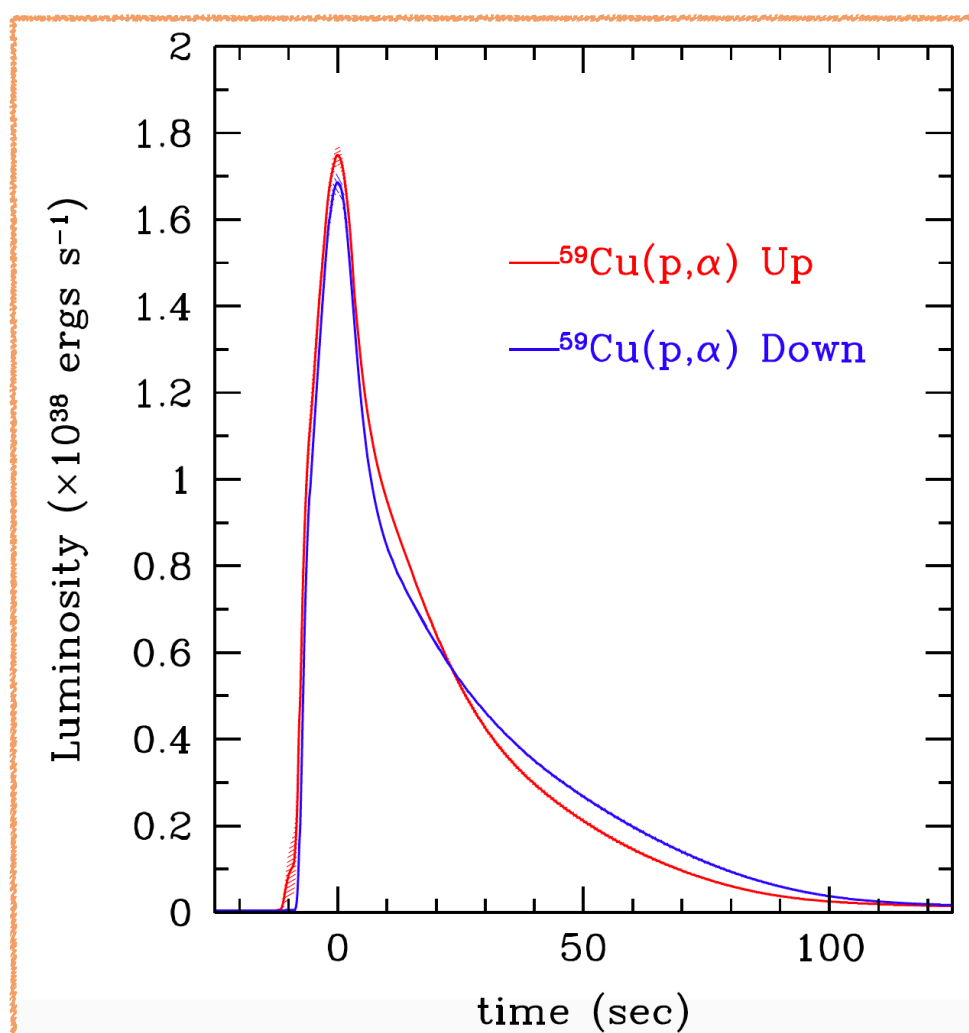


Table 2

Reactions that Impact the Burst Light Curve
in the Multi-zone X-ray Burst Model

Rank	Reaction	Type ^a	Sensitivity ^b	Category
1	$^{15}\text{O}(\alpha, \gamma)^{19}\text{Ne}$	D	16	1
2	$^{56}\text{Ni}(\alpha, p)^{59}\text{Cu}$	U	6.4	1
3	$^{59}\text{Cu}(p, \gamma)^{60}\text{Zn}$	D	5.1	1
4	$^{61}\text{Ga}(p, \gamma)^{62}\text{Ge}$	D	3.7	1
5	$^{22}\text{Mg}(\alpha, p)^{25}\text{Al}$	D	2.3	1
6	$^{14}\text{O}(\alpha, p)^{17}\text{F}$	D	5.8	1
7	$^{23}\text{Al}(p, \gamma)^{24}\text{Si}$	D	4.6	1
8	$^{18}\text{Ne}(\alpha, p)^{21}\text{Na}$	U	1.8	1
9	$^{63}\text{Ga}(p, \gamma)^{64}\text{Ge}$	D	1.4	2
10	$^{19}\text{F}(p, \alpha)^{16}\text{O}$	U	1.3	2

Multi-zone model results

Astrophysical Motivation

X-ray Bursts (ash composition)

Multi-zone model results

- Inverse of $^{59}\text{Cu}(p, \alpha)$ reaction affects the composition of the burst ashes (*R. Cyburt et al, ApJ 830, 2016*)

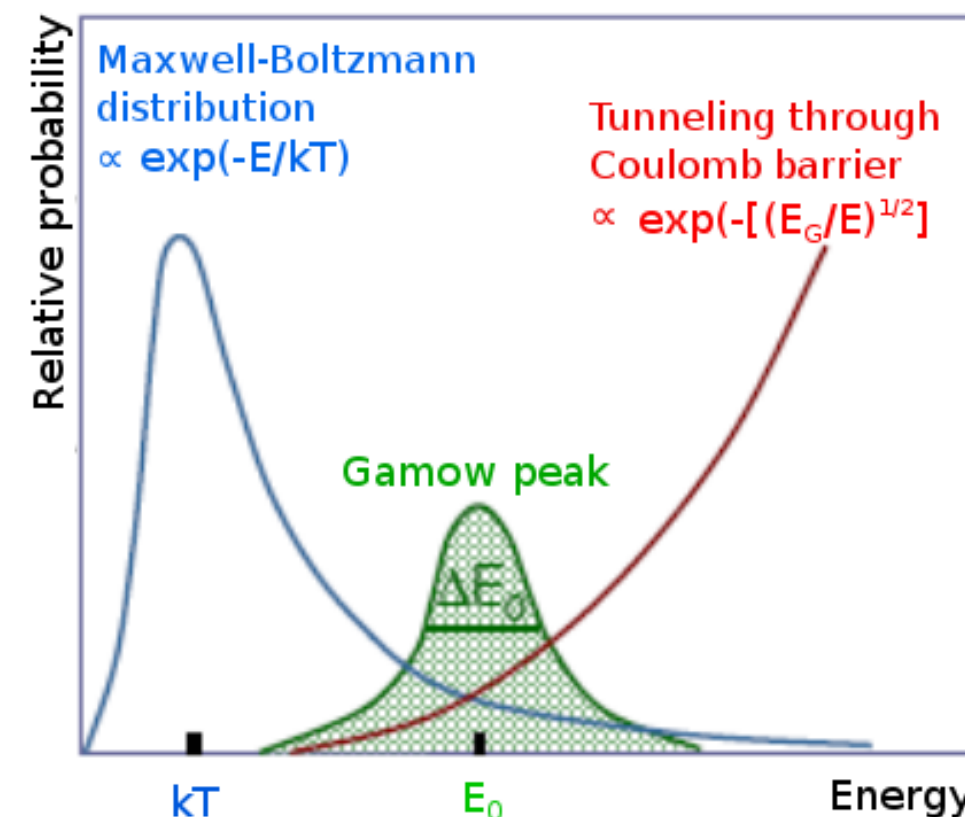
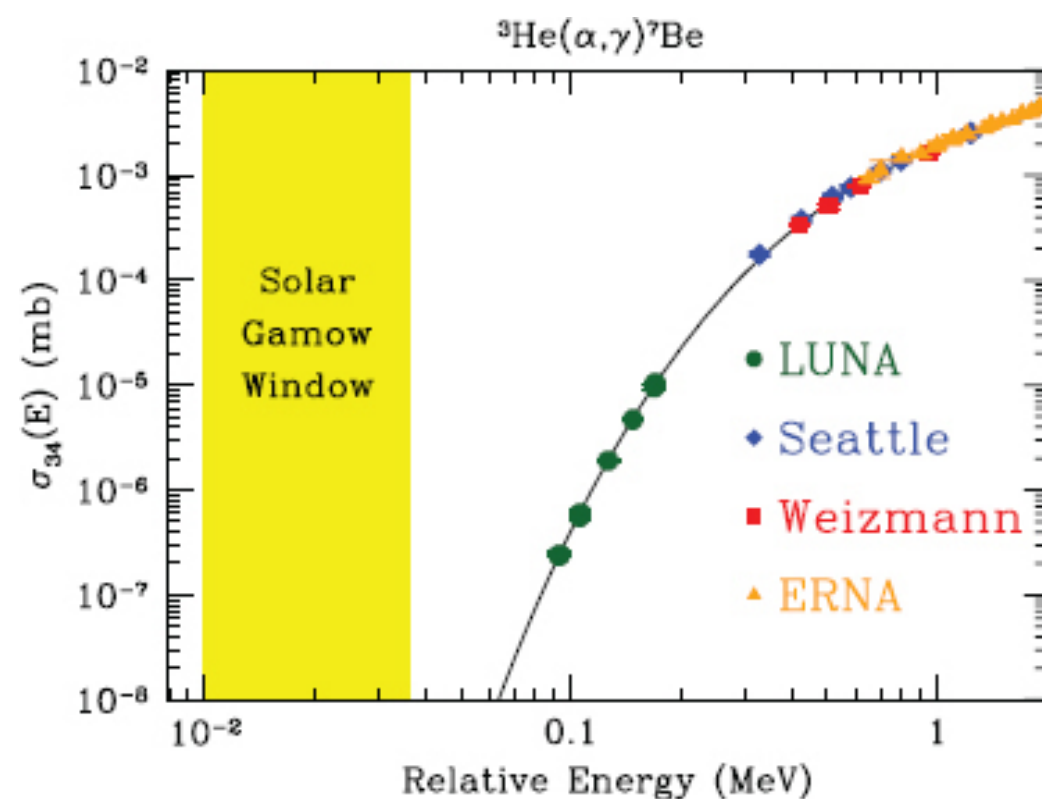
Table 5
Reactions that Impact the Composition in the Multi-zone X-Ray Burst Model

Count	Reaction	Max. Ratio ^a	Affected Mass Numbers with Mass Fraction $> 10^{-4}$		
			max	$> \times 10$ change	$\times 2 < \text{change}$ $< \times 10$
1	$^8\text{Be}(\alpha, \gamma)^{12}\text{C}$	3	98		30, 93–99
2	$^{12}\text{C}(\alpha, \gamma)^{16}\text{O}$	2	28		28
3	$^{14}\text{O}(\alpha, p)^{17}\text{F}$	4	29		29
⋮	⋮	⋮	⋮		⋮
23	$^{54}\text{Fe}(p, \gamma)^{55}\text{Co}$	6	54		54
24	$^{56}\text{Ni}(\alpha, p)^{59}\text{Cu}$	5	29		12, 29–30, 56, 75, 78–79, 82
25	$^{59}\text{Cu}(p, \gamma)^{60}\text{Zn}$	200	59	59	12, 29–30, 75, 78–79

Experimental Measurement

Gamow Window: The relevant energy range for any stellar environment.

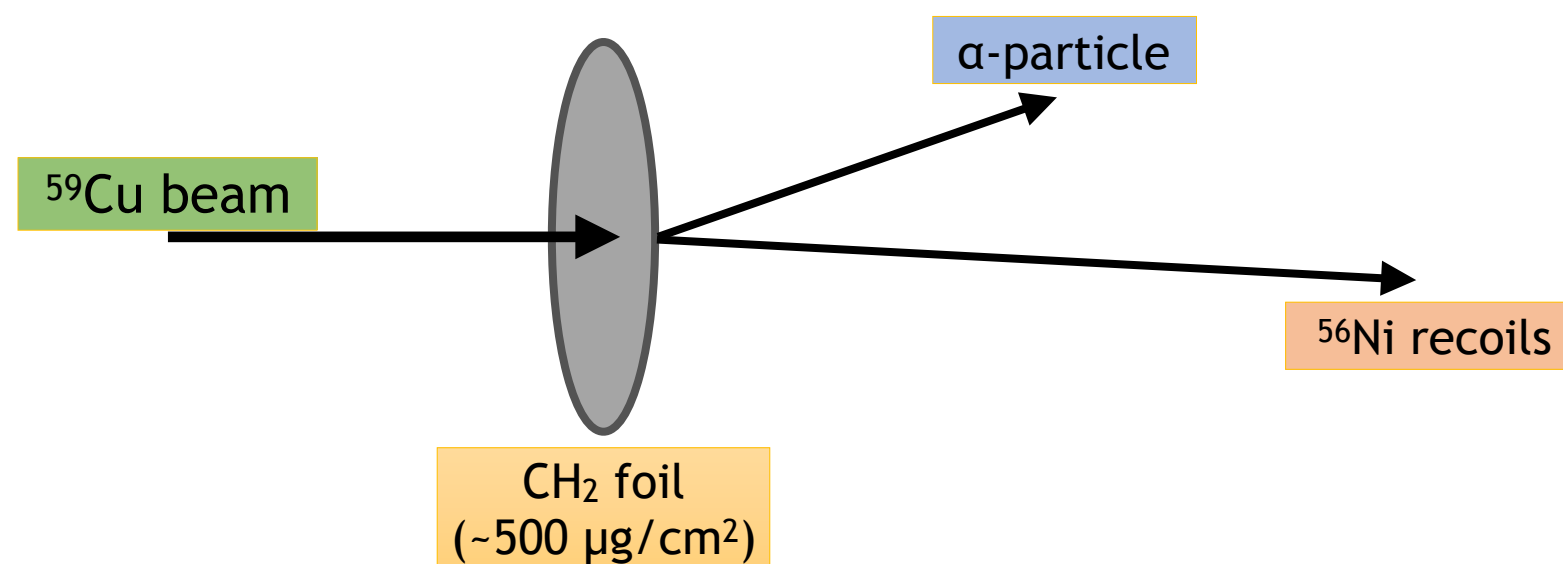
The reaction probability (cross-section, $\sigma(E)$) falls rapidly at lower energies!!



Challenge: The direct measurements in this energy range are not easy

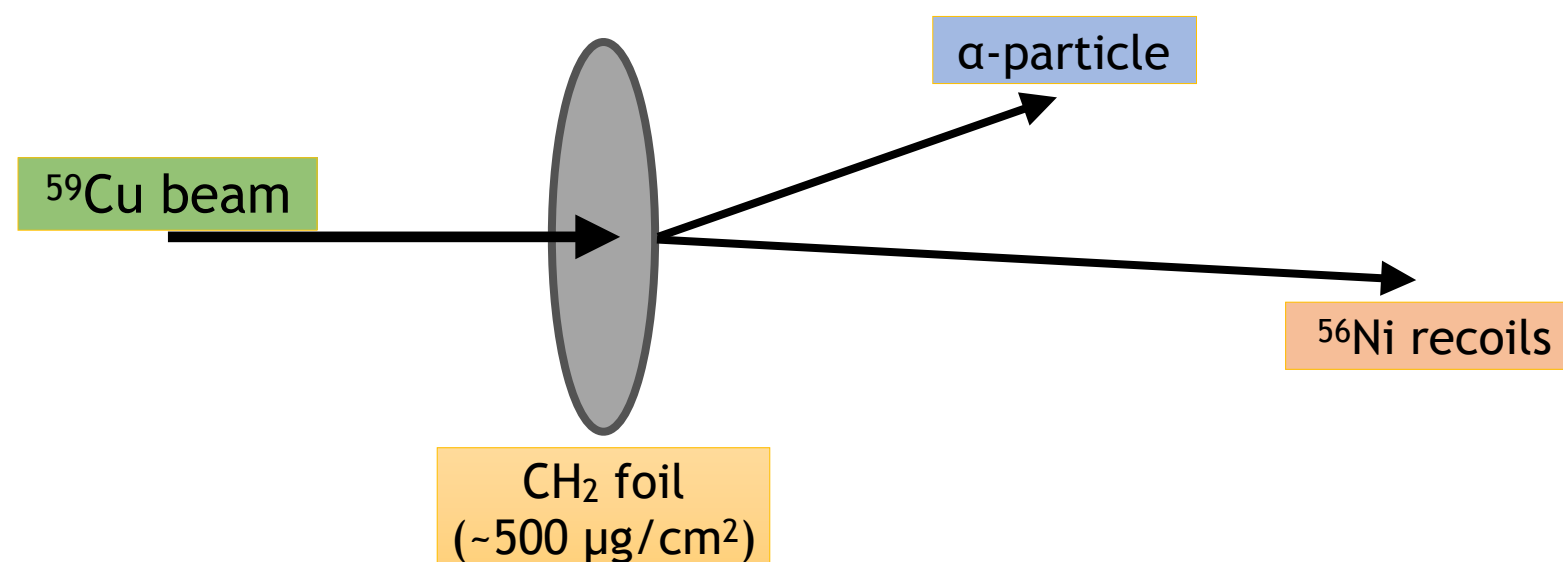
Experimental Setup

$^{59}\text{Cu}(p,\alpha)^{56}\text{Ni}$ reaction studied in inverse kinematics



Experimental Setup

$^{59}\text{Cu}(p,\alpha)^{56}\text{Ni}$ reaction studied in inverse kinematics

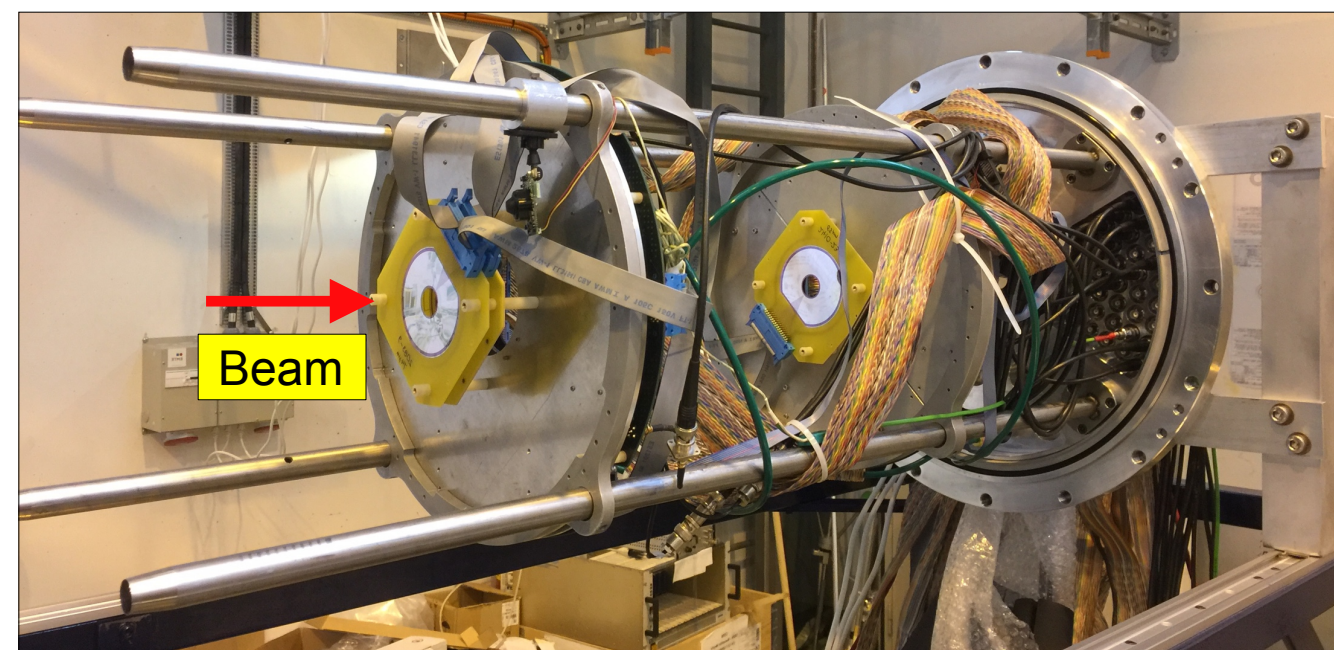
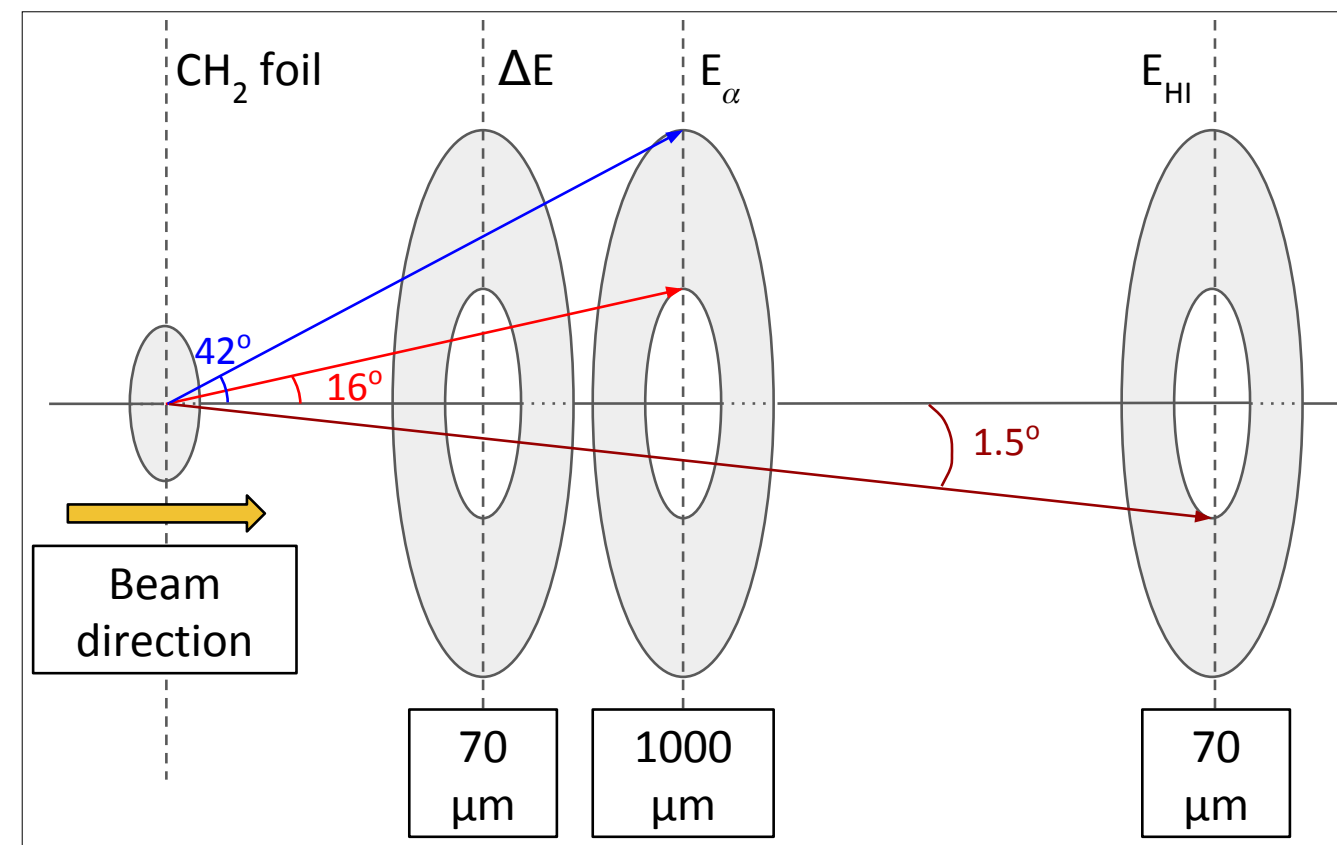


Radioactive ^{59}Cu beam delivered by HIE-ISOLDE at CERN

- Intensity $\sim 2 \text{ epA}$ ($5.5 \times 10^5 \text{ pps}$)
- High purity
- 5 different energies between 3.6 - 5.0 MeV/u

Experimental Setup

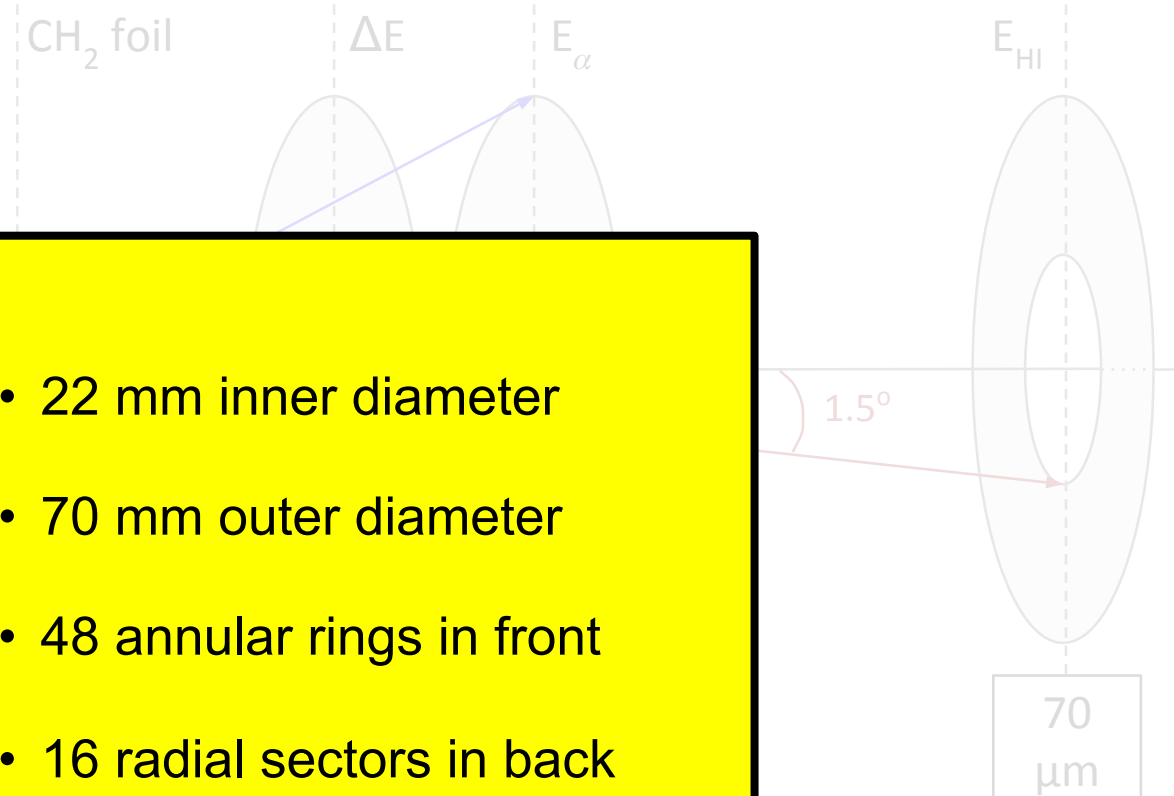
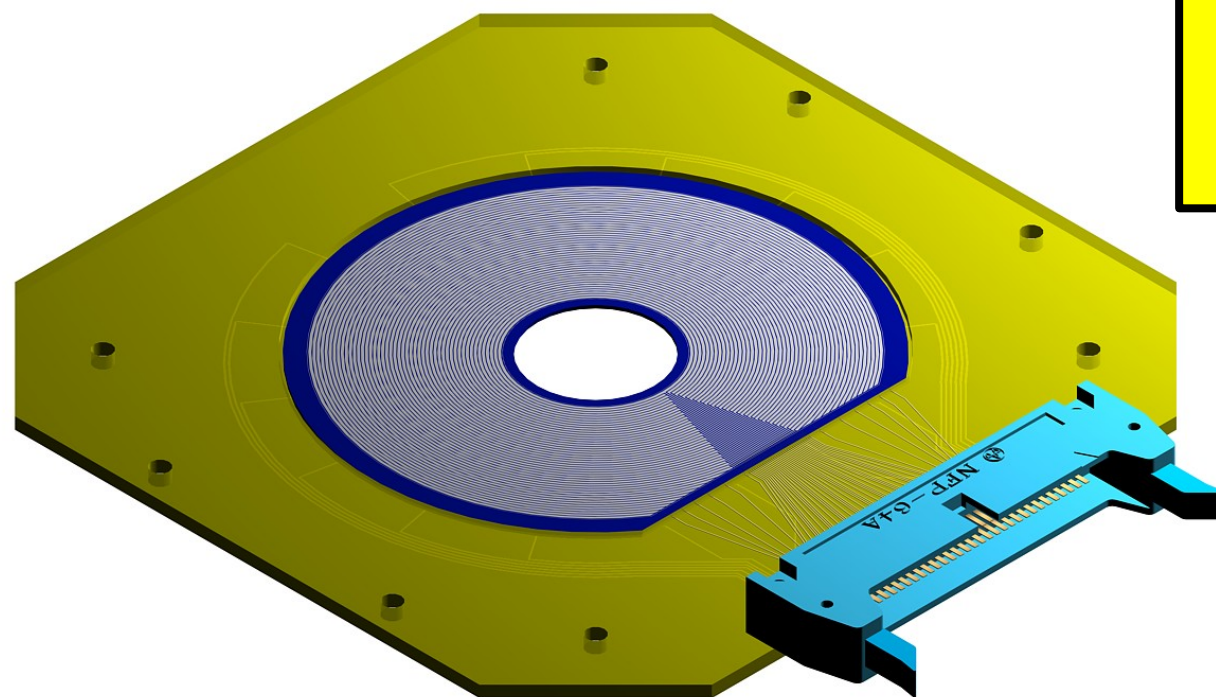
- The reaction products were detected using S2-type silicon detector array (purpose-built by University of Edinburgh)



Experimental Setup

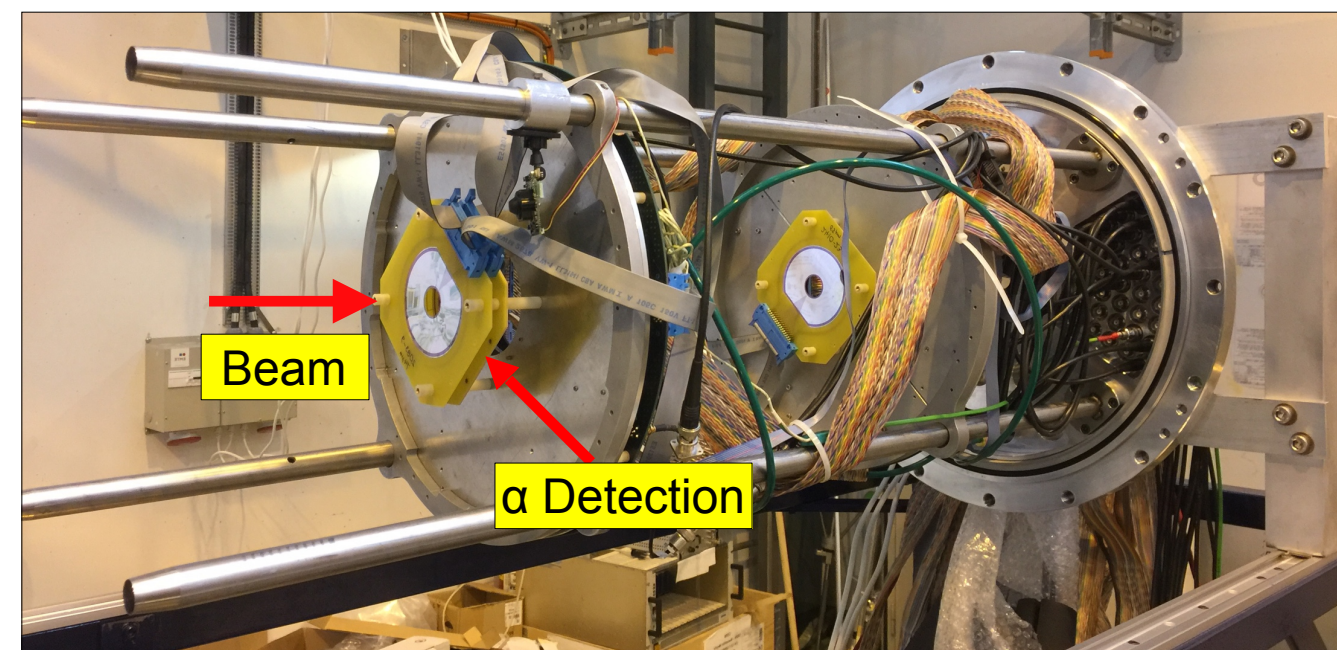
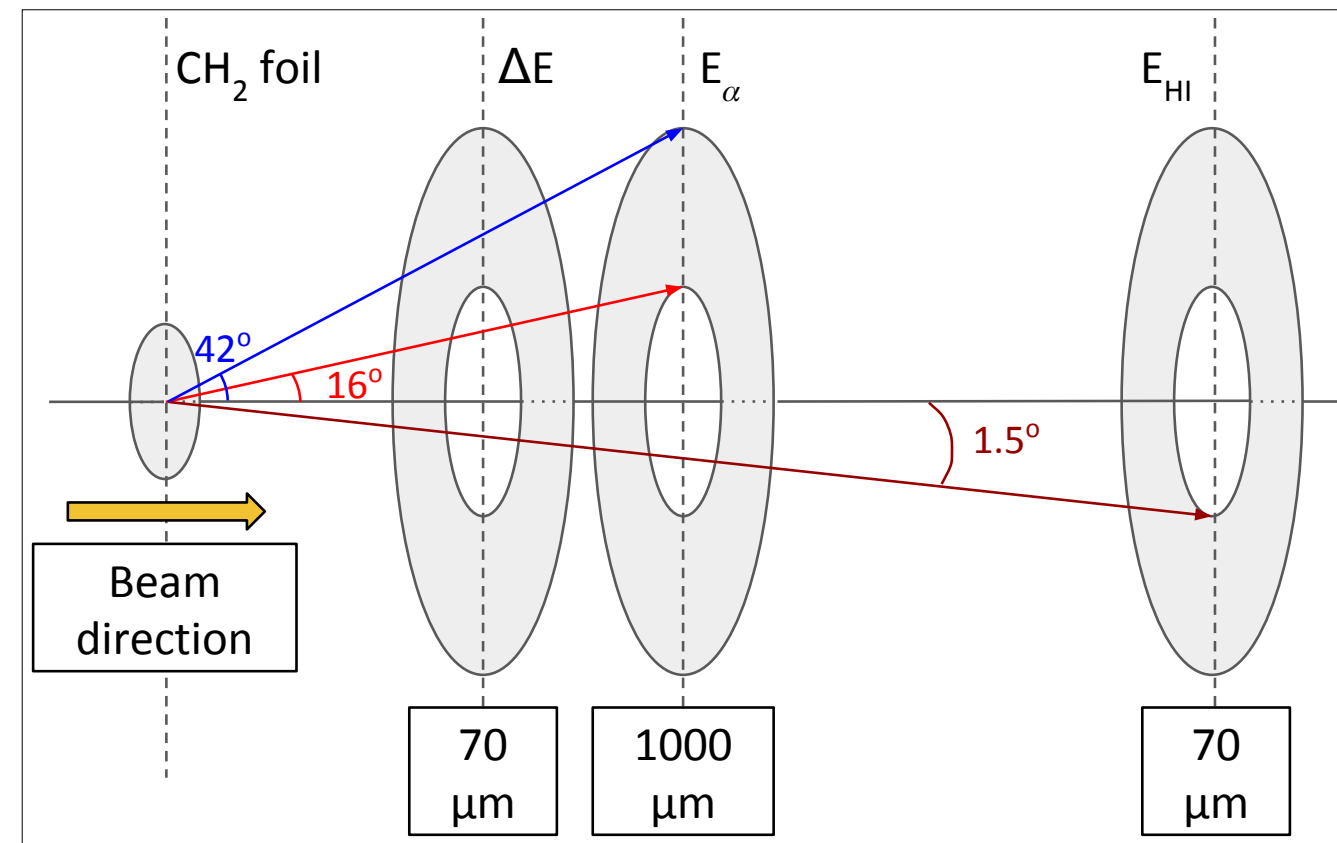
- The reaction products were detected using **S2-type silicon detector array** (purpose-built by University of Edinburgh)

- 22 mm inner diameter
- 70 mm outer diameter
- 48 annular rings in front
- 16 radial sectors in back



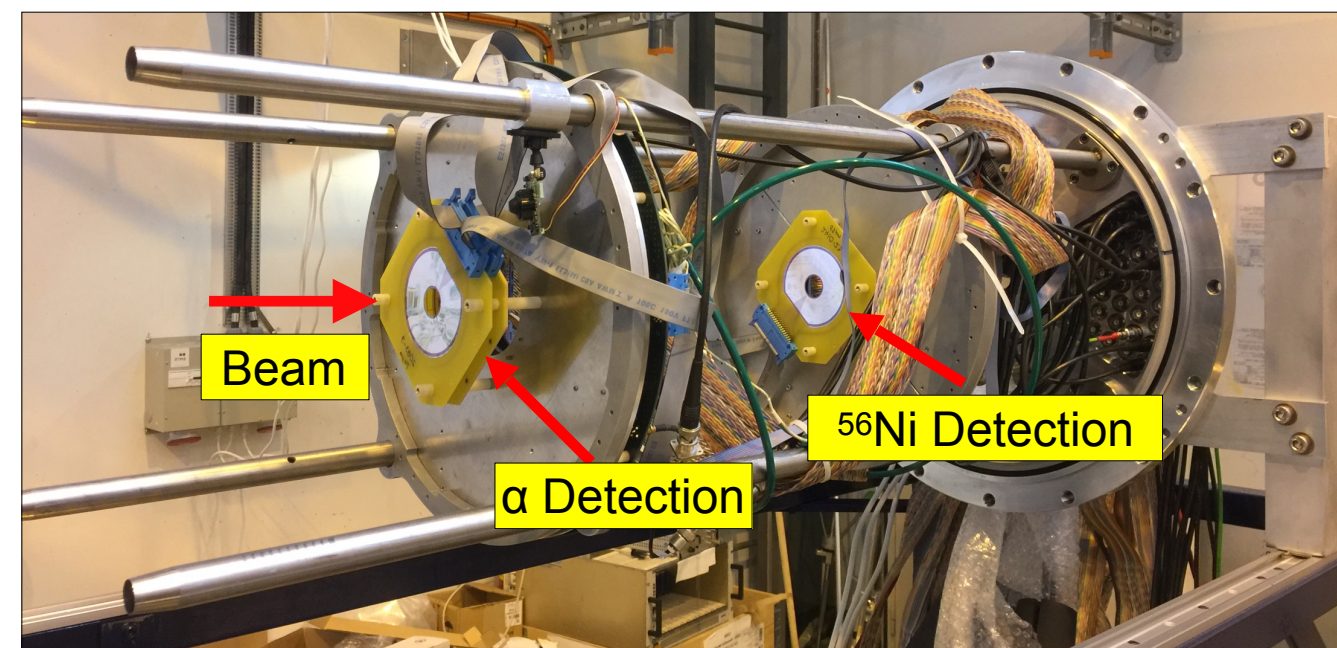
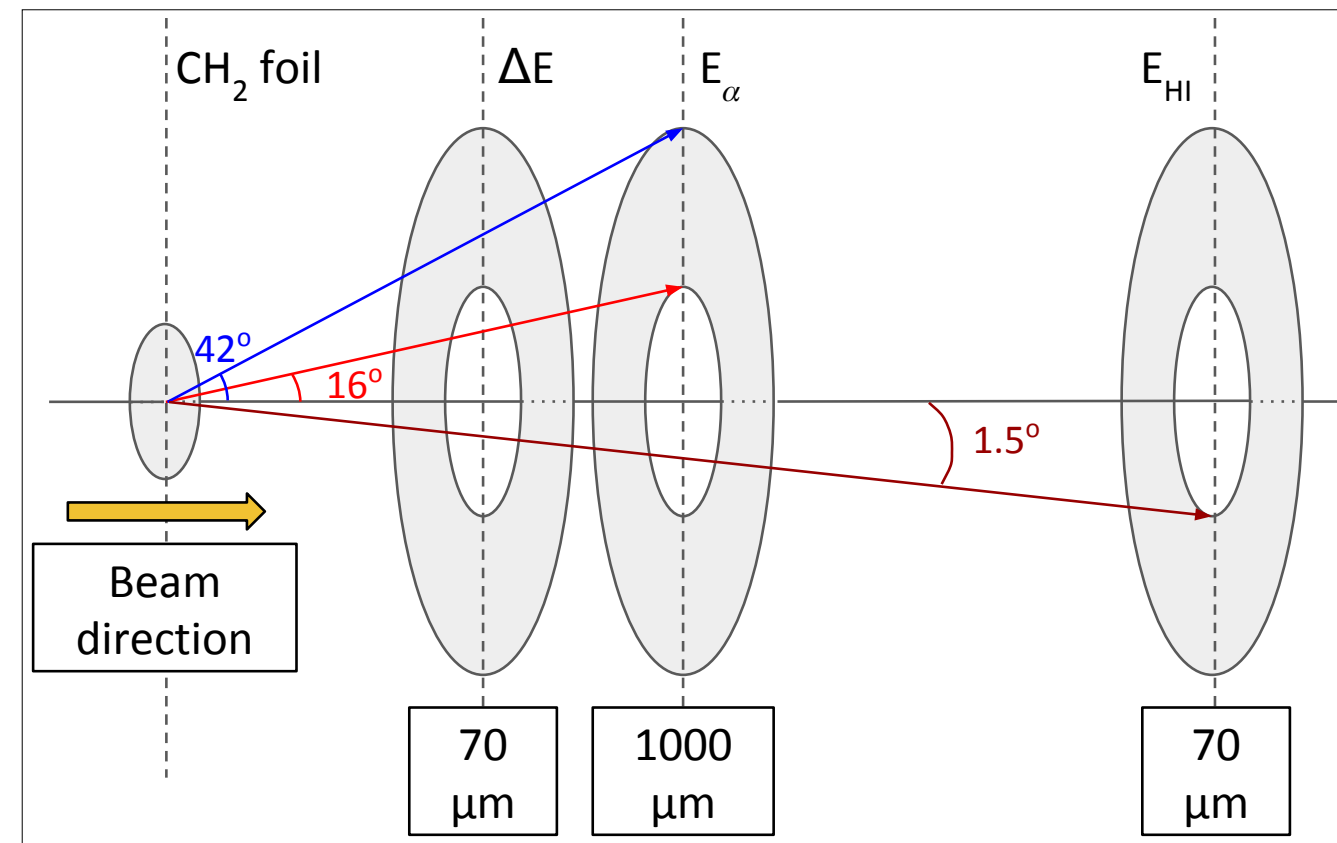
Experimental Setup

- The reaction products were detected using S2-type silicon detector array (purpose-built by University of Edinburgh)
- ΔE -E telescope placed at 30 mm from target to cover large lab-angles for α -particles detection.



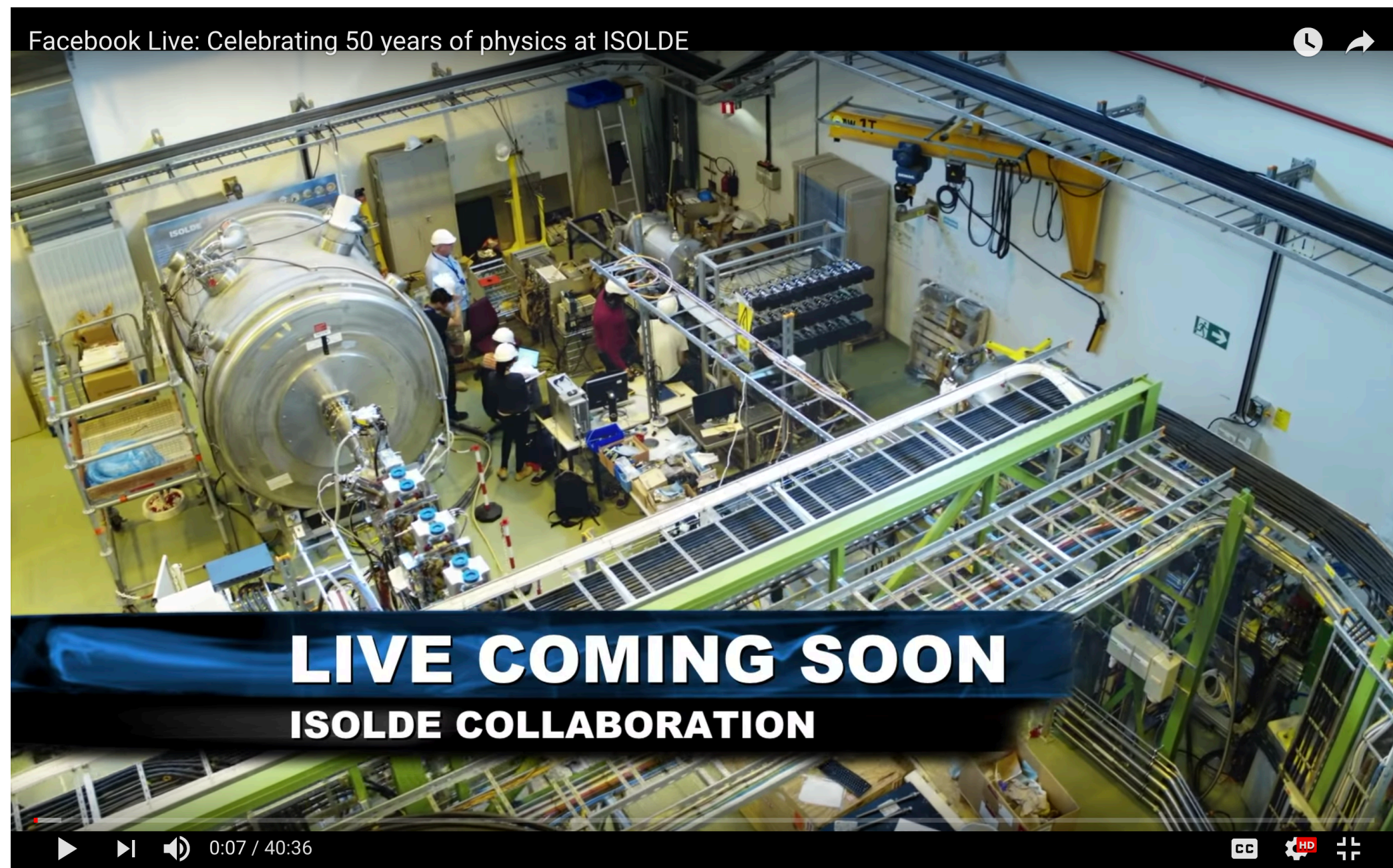
Experimental Setup

- The reaction products were detected using S2-type silicon detector array (purpose-built by **University of Edinburgh**)
- ΔE -E telescope placed at 30 mm from target to cover large lab-angles for α -particles detection.
- ^{56}Ni recoils detector was placed at 400 mm to cover forward angles.



Data Analysis

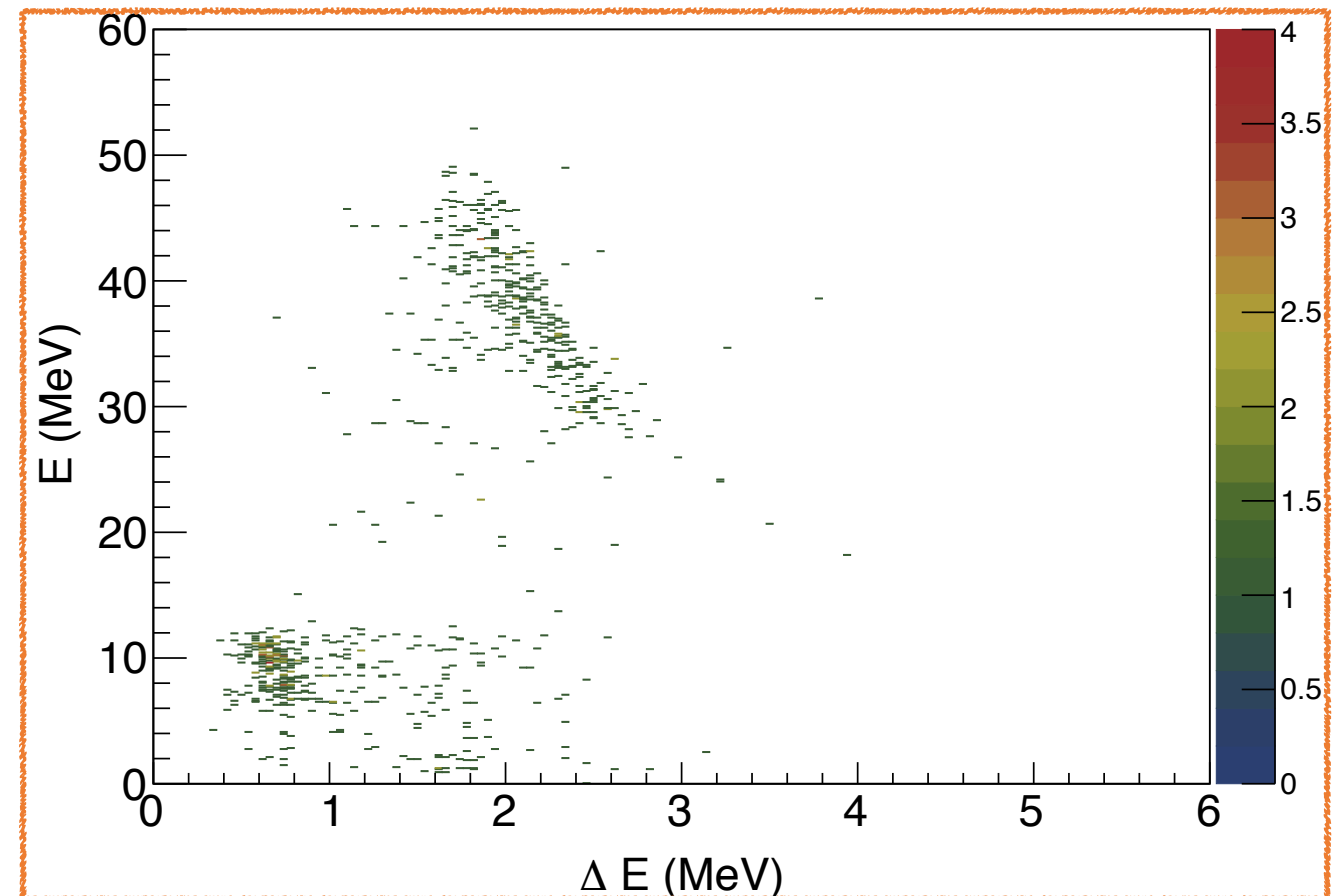
Extra stuff: ISOLDE's 50 year anniversary [video](#)



Data Analysis

Coincidence detection of reaction products (α -particle and ^{56}Ni)

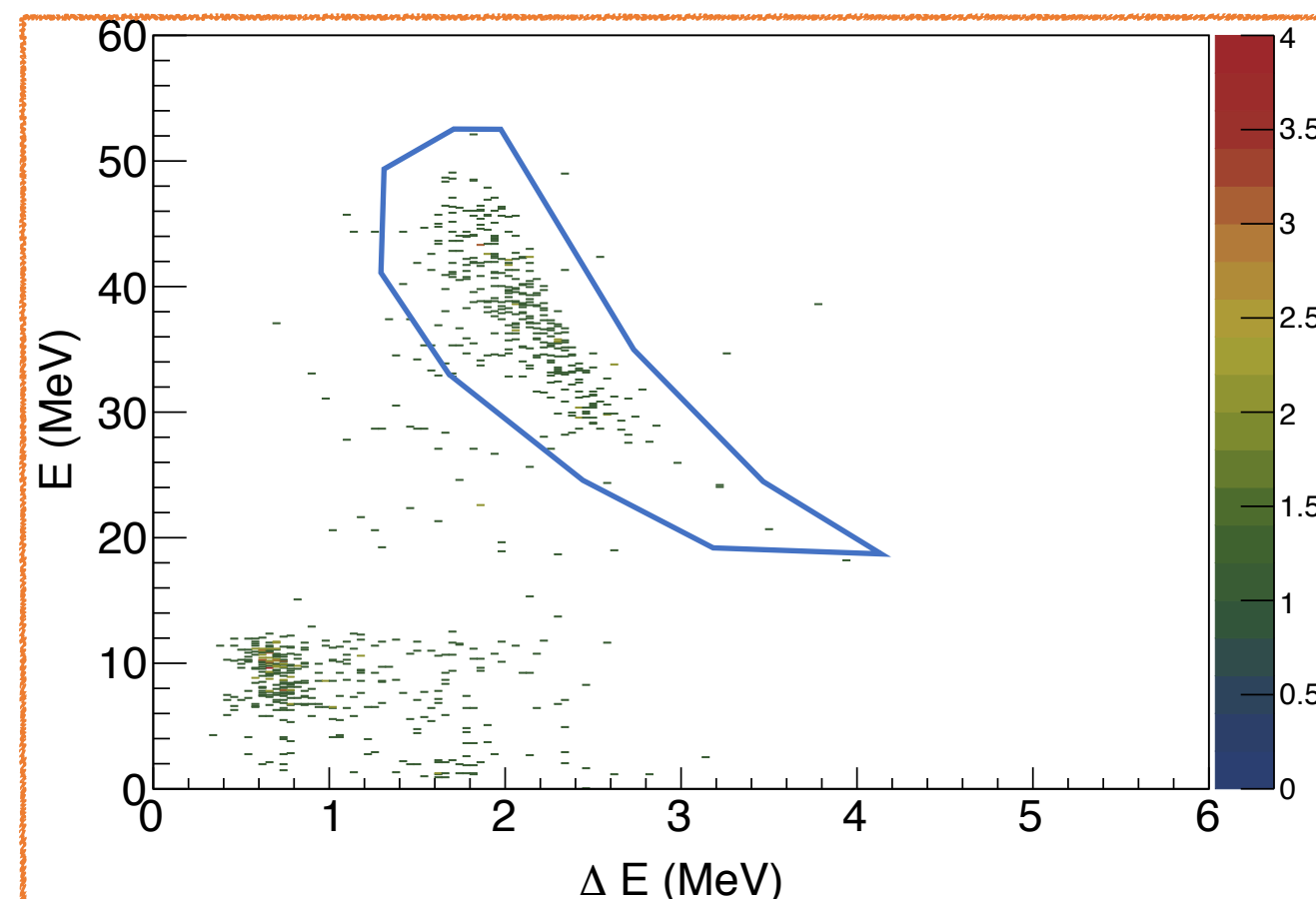
- α -particle detected using the ΔE -E telescope
- The α -particle identification done using the E vs ΔE plot



Data Analysis

Coincidence detection of reaction products (α -particle and ^{56}Ni)

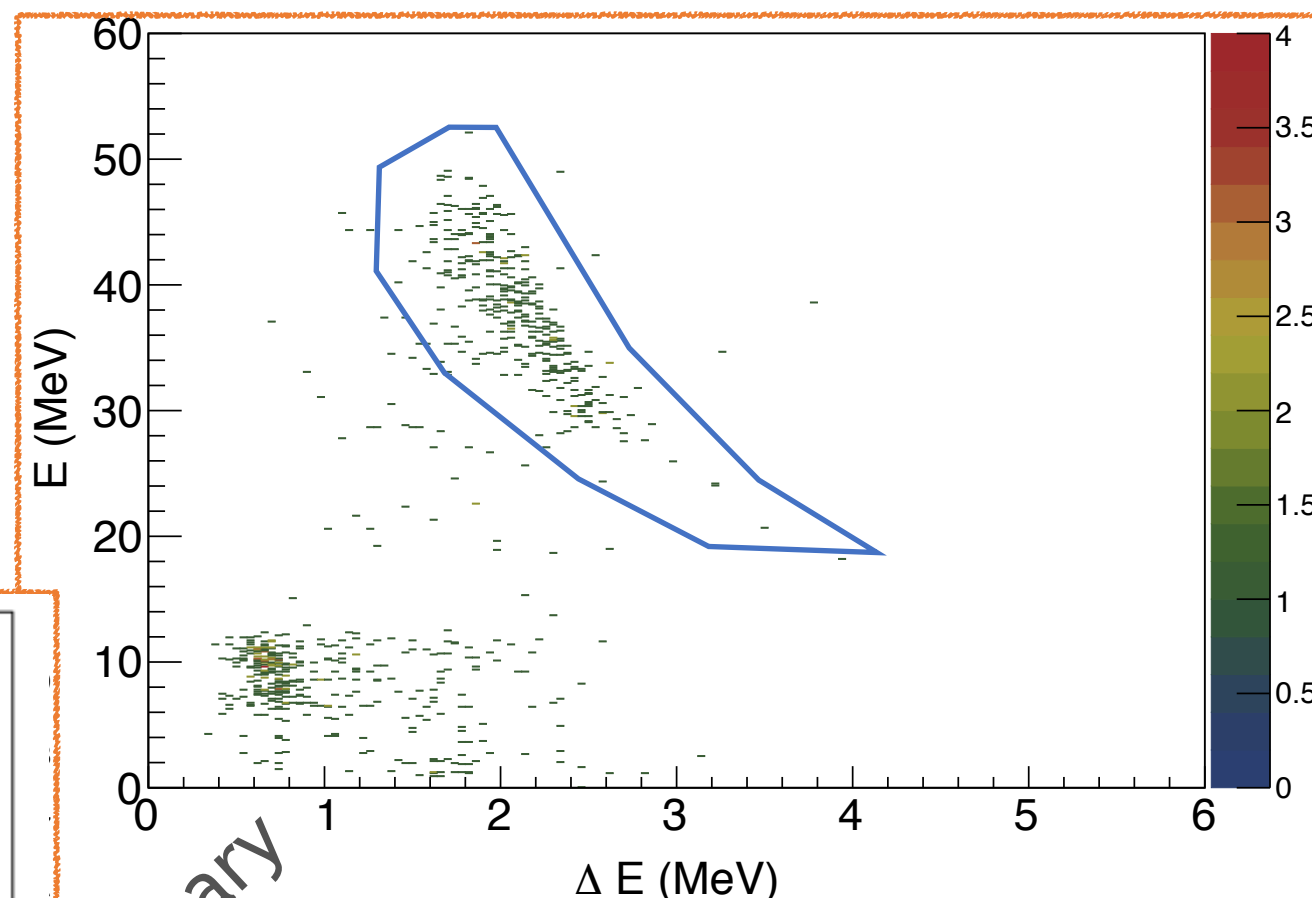
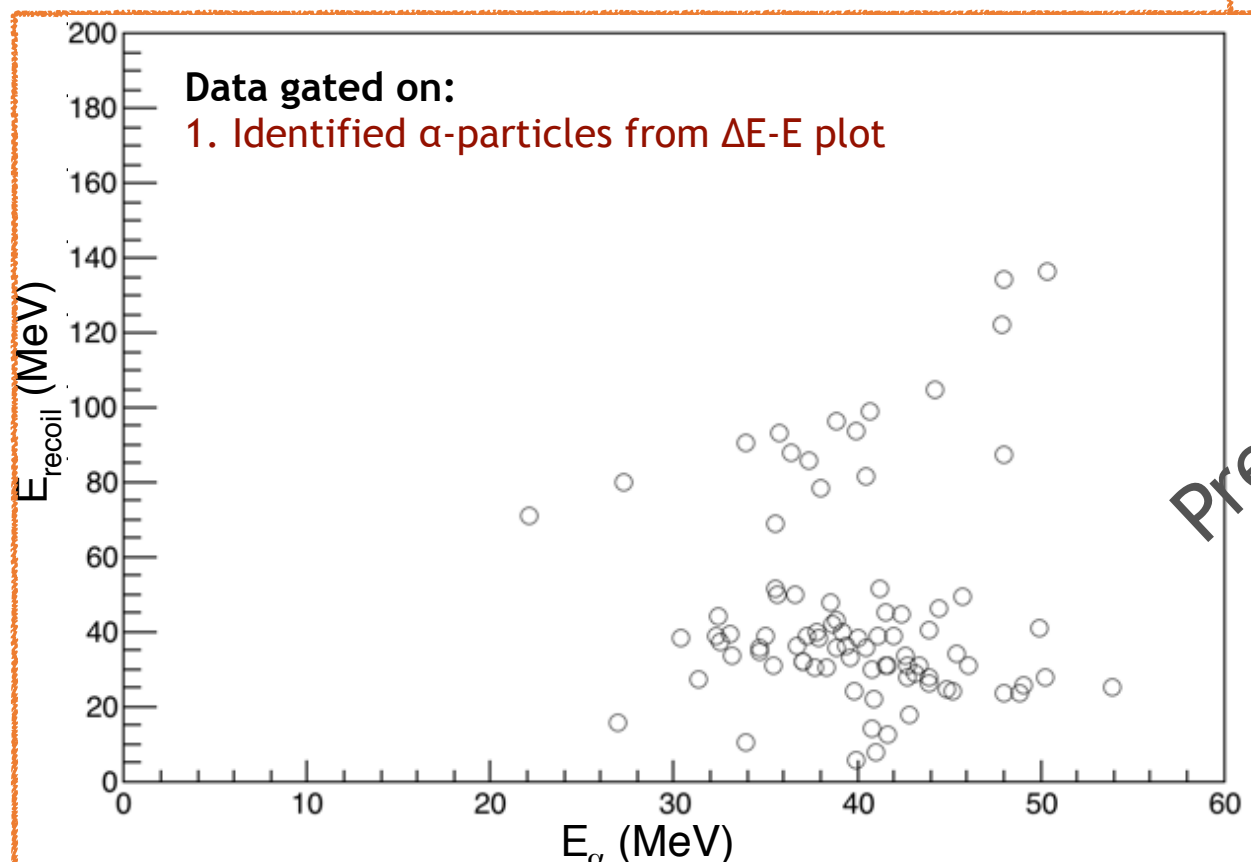
- α -particle detected using the ΔE -E telescope
- The α -particle identification done using the E vs ΔE plot



Data Analysis

Coincidence detection of reaction products (α -particle and ^{56}Ni)

- α -particle detected using the ΔE -E telescope
- The α -particle identification done using the E vs ΔE plot



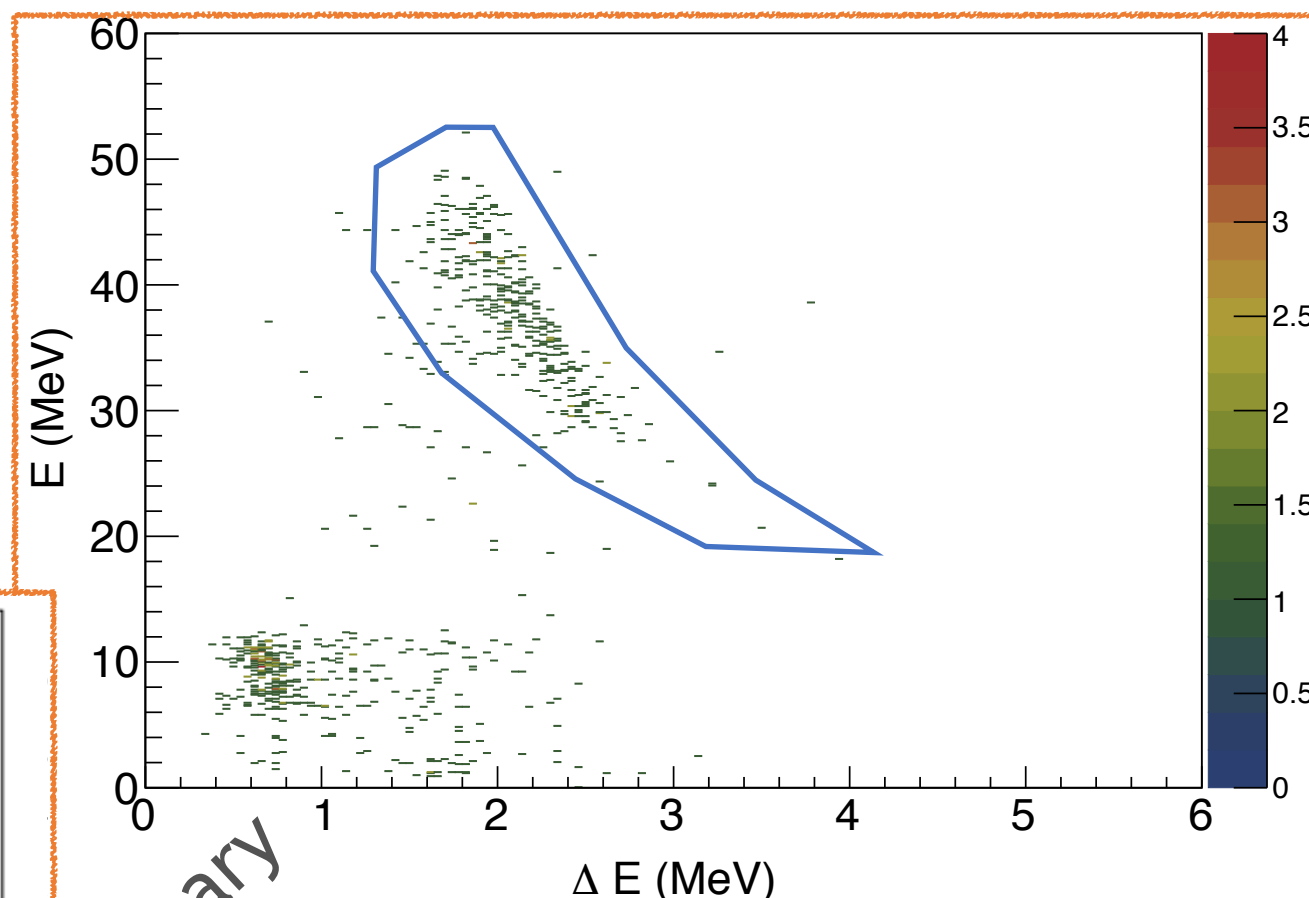
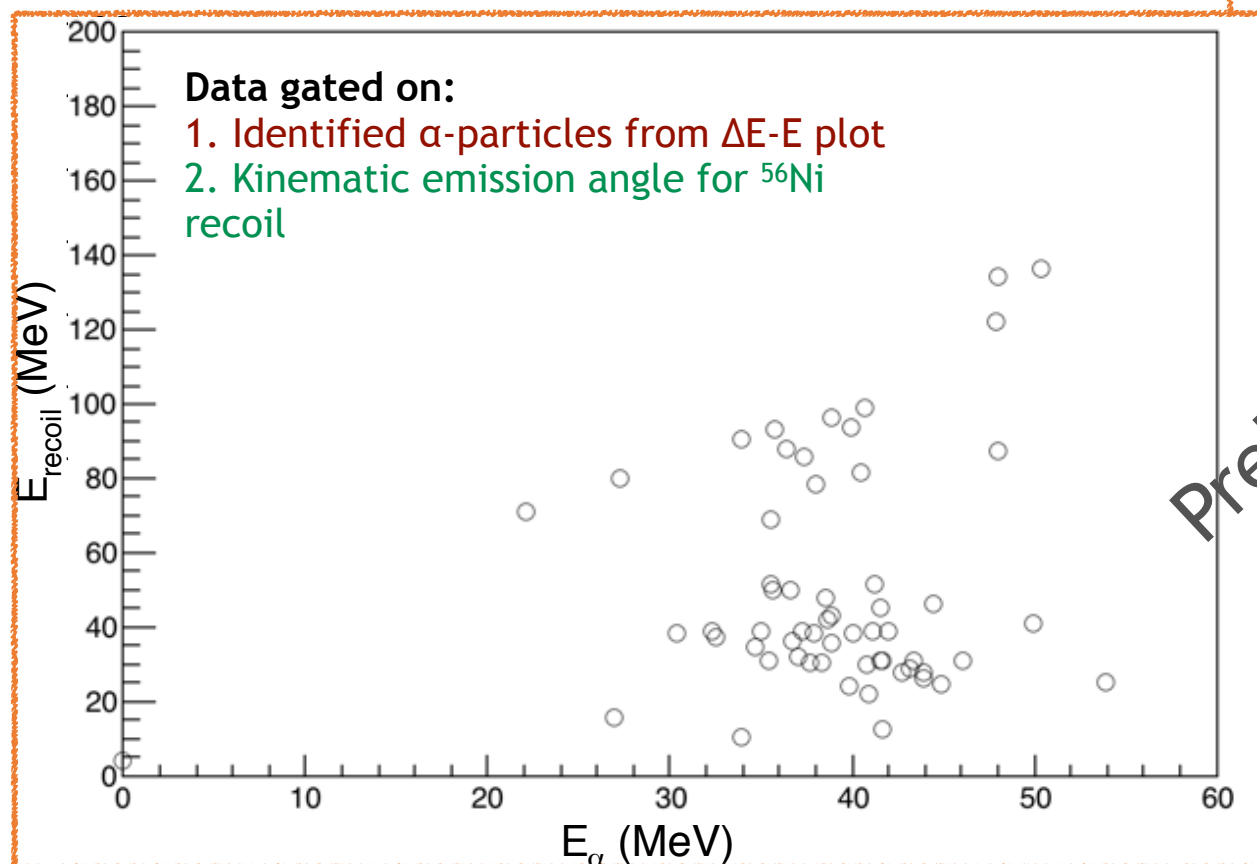
Preliminary

- Identified α -particle's energy is plotted against HI energies
- The background events are cut out by gating data on momentum

Data Analysis

Coincidence detection of reaction products (α -particle and ^{56}Ni)

- α -particle detected using the ΔE -E telescope
- The α -particle identification done using the E vs ΔE plot



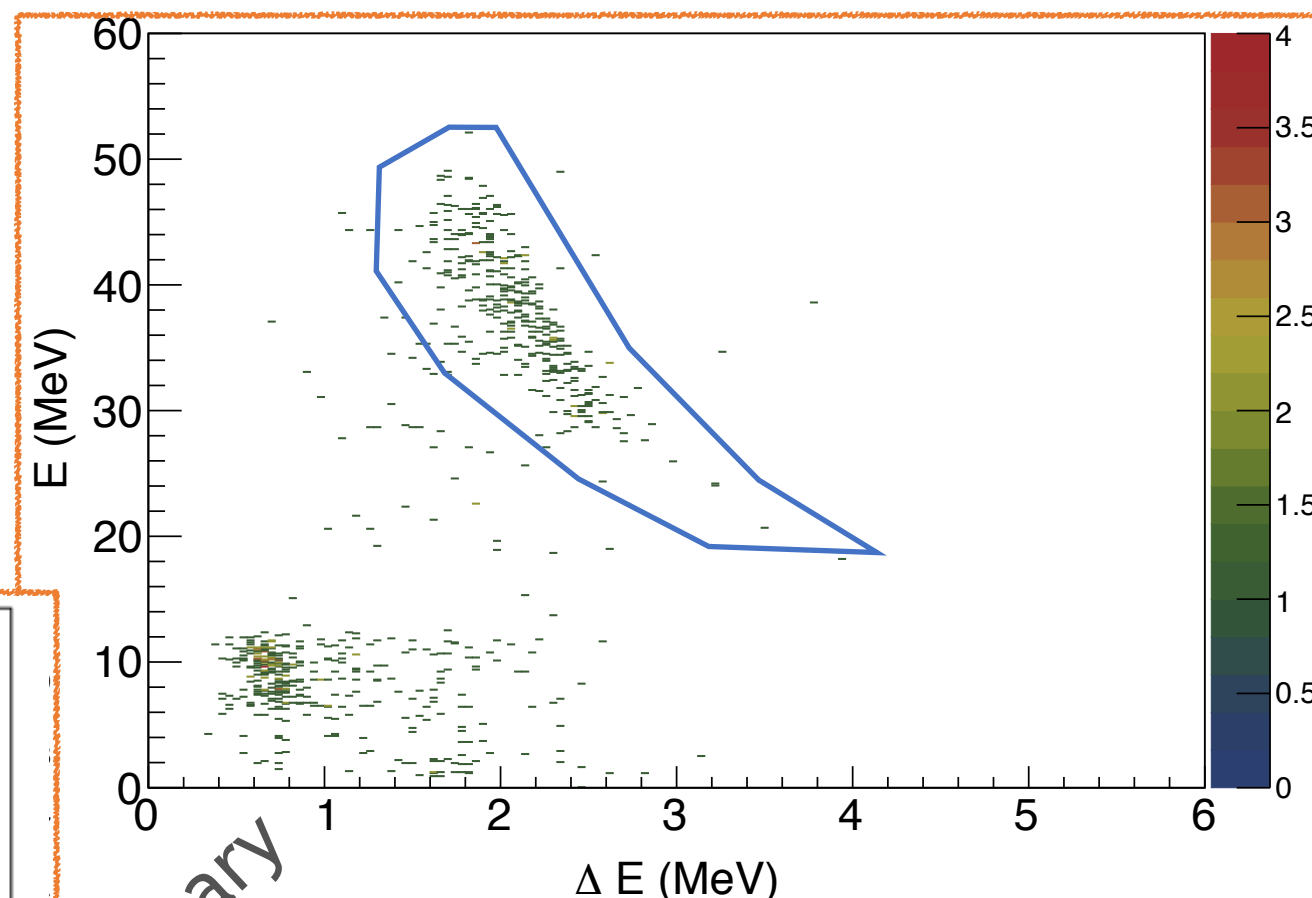
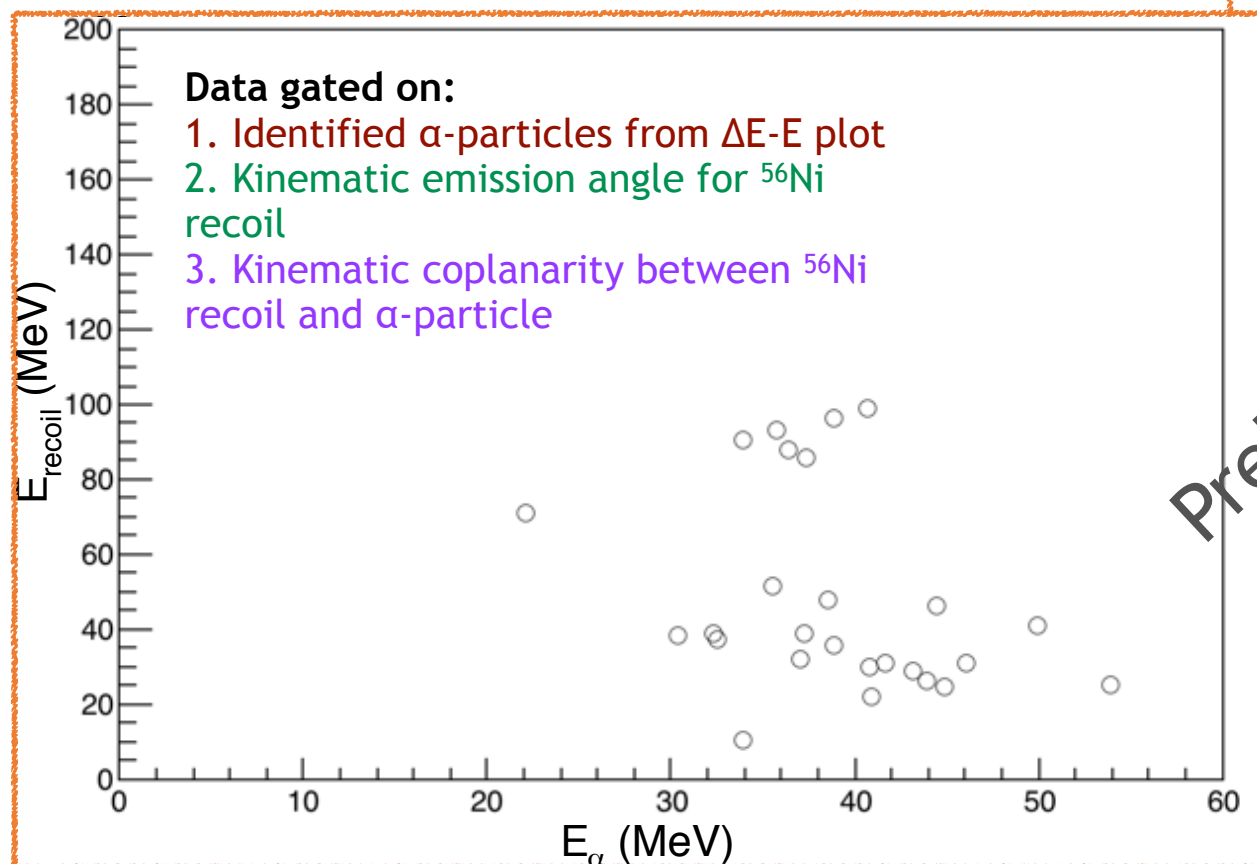
Preliminary

- Identified α -particle's energy is plotted against HI energies
- The background events are cut out by gating data on momentum

Data Analysis

Coincidence detection of reaction products (α -particle and ^{56}Ni)

- α -particle detected using the ΔE -E telescope
- The α -particle identification done using the E vs ΔE plot



- Identified α -particle's energy is plotted against HI energies
- The background events are cut out by gating data on momentum

Data Analysis

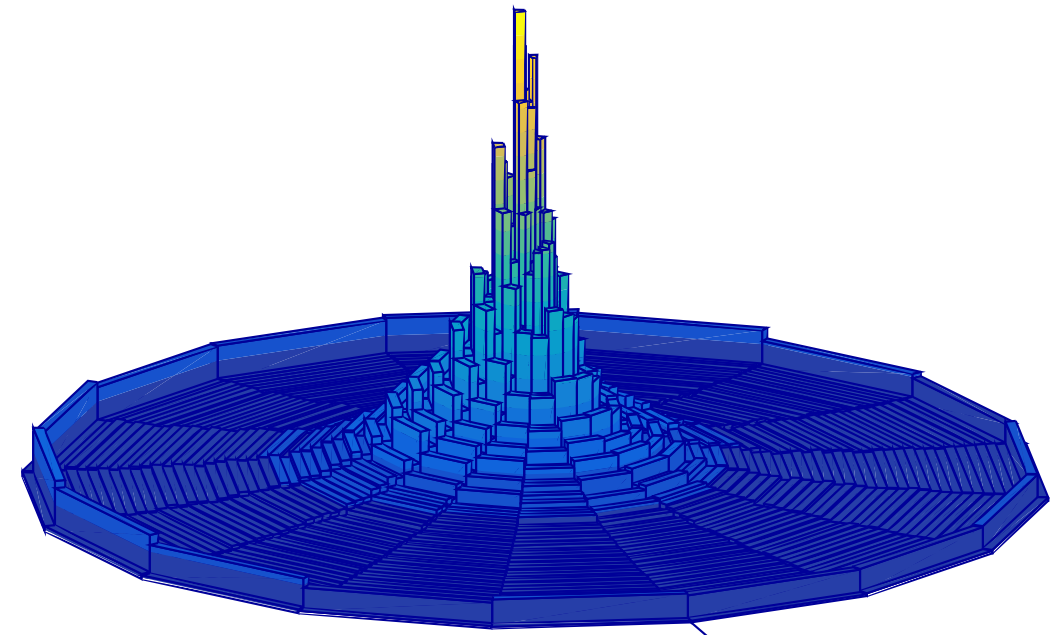
Beam intensity measurement

- Faraday cup reading at the end of the detector setup

Data Analysis

Beam intensity measurement

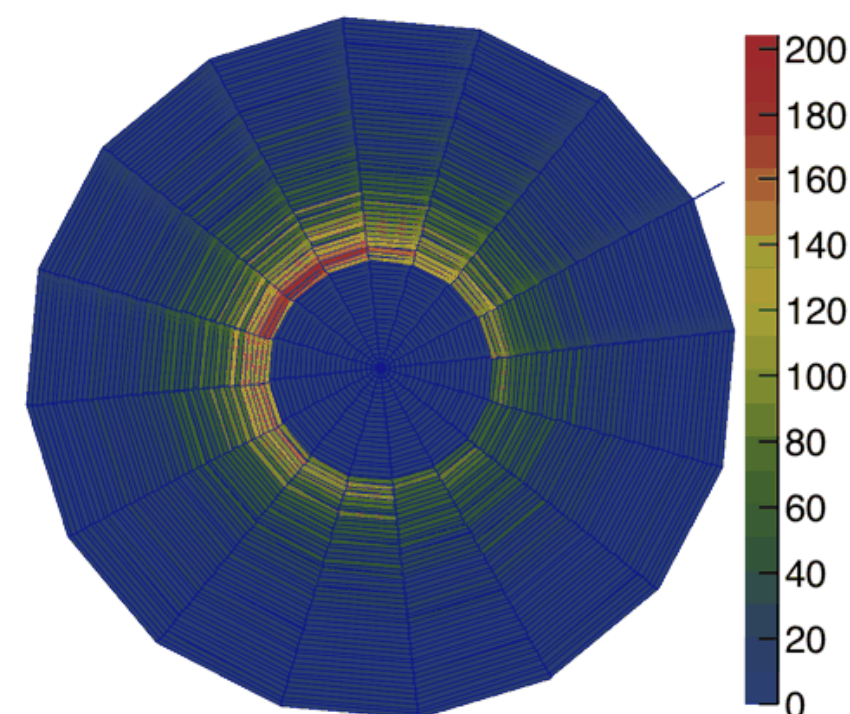
- Faraday cup reading at the end of the detector setup
- Rutherford scattering of ^{59}Cu on ^{12}C in the target foil



Data Analysis

Beam intensity measurement

- Faraday cup reading at the end of the detector setup
- Rutherford scattering of ^{59}Cu on ^{12}C in the target foil



R147, E_{beam} = 5.0 MeV/u

Calculated beam current: 7.7 pA

FC reading: 2.1 pA

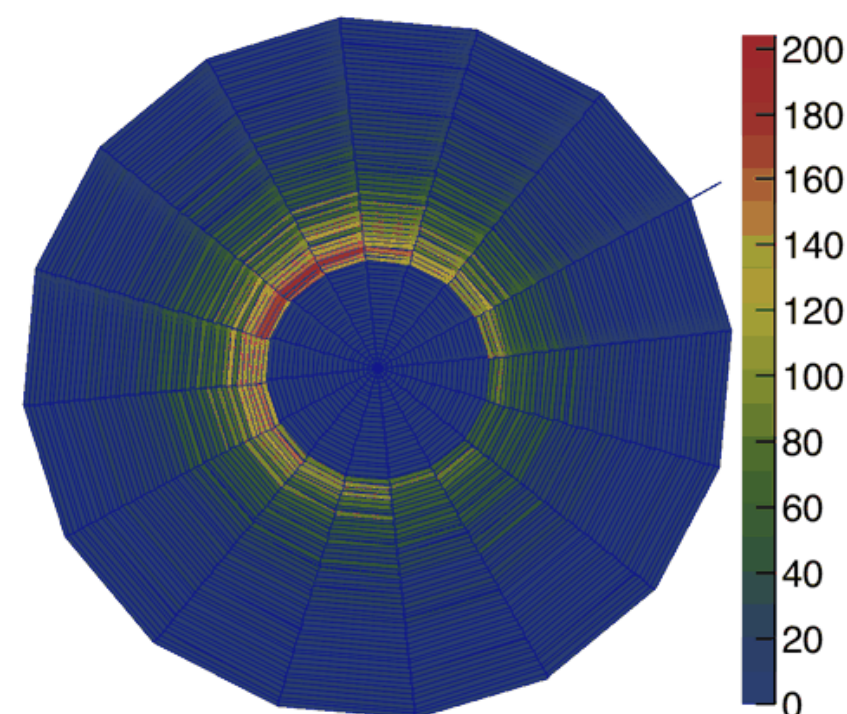
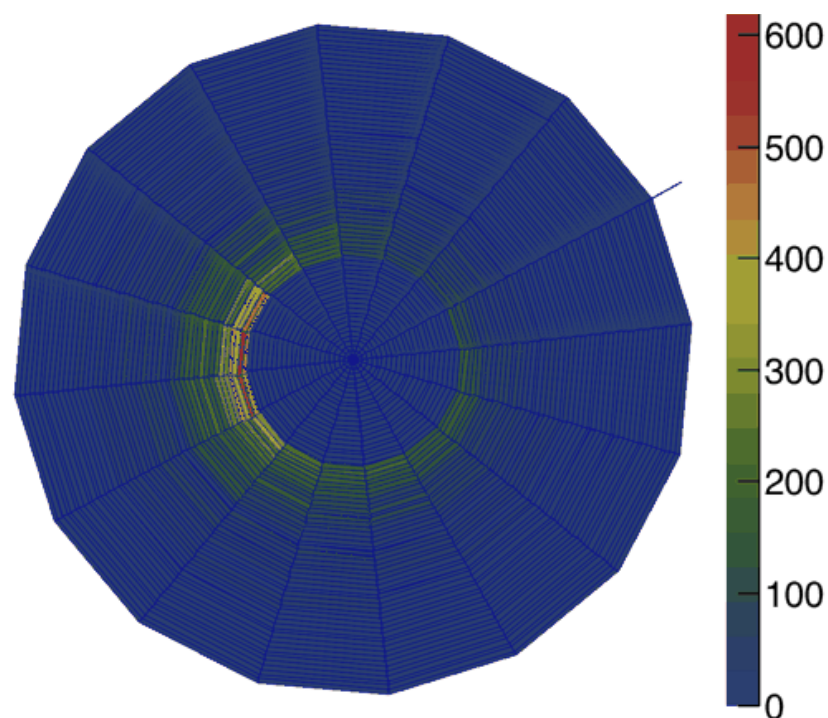
Data Analysis

Beam intensity measurement

- Faraday cup reading at the end of the detector setup
- Rutherford scattering of ^{59}Cu on ^{12}C in the target foil

R77, E_beam = 4.7 MeV/u

Calculated beam current: 9.0 pA
FC reading: 1.85 pA



R147, E_beam = 5.0 MeV/u

Calculated beam current: 7.7 pA
FC reading: 2.1 pA

Summary I: The $^{59}\text{Cu}(p,\alpha)^{56}\text{Ni}$ measurement

- $^{59}\text{Cu}(p,\alpha)^{56}\text{Ni}$ reaction cross section has implications on:
 - P-nuclei production in core collapse supernovae
 - X-ray burst light curve
 - X-ray burst ash compositions
- No experimental data available on direct measurement
- First direct measurement performed by University of Edinburgh group at HIE-ISOLDE, CERN
- Data analysis - 'work in progress'

Thank you for your attention!